

## Geological Society of America Bulletin

### The chronology of the Eocene tectonic and stratigraphic development of the eastern Pyrenean foreland basin, northeast Spain

DOUGLAS W. BURBANK, CAI PUIGDEFÀBREGAS and JOSEP ANTON MUÑOZ

*Geological Society of America Bulletin* 1992;104, no. 9;1101-1120  
doi: 10.1130/0016-7606(1992)104<1101:TCOTET>2.3.CO;2

---

**Email alerting services** click [www.gsapubs.org/cgi/alerts](http://www.gsapubs.org/cgi/alerts) to receive free e-mail alerts when new articles cite this article

**Subscribe** click [www.gsapubs.org/subscriptions/](http://www.gsapubs.org/subscriptions/) to subscribe to Geological Society of America Bulletin

**Permission request** click <http://www.geosociety.org/pubs/copyrt.htm#gsa> to contact GSA

Copyright not claimed on content prepared wholly by U.S. government employees within scope of their employment. Individual scientists are hereby granted permission, without fees or further requests to GSA, to use a single figure, a single table, and/or a brief paragraph of text in subsequent works and to make unlimited copies of items in GSA's journals for noncommercial use in classrooms to further education and science. This file may not be posted to any Web site, but authors may post the abstracts only of their articles on their own or their organization's Web site providing the posting includes a reference to the article's full citation. GSA provides this and other forums for the presentation of diverse opinions and positions by scientists worldwide, regardless of their race, citizenship, gender, religion, or political viewpoint. Opinions presented in this publication do not reflect official positions of the Society.

---

#### Notes

# The chronology of the Eocene tectonic and stratigraphic development of the eastern Pyrenean foreland basin, northeast Spain

DOUGLAS W. BURBANK *Department of Geological Sciences, University of Southern California, Los Angeles, California 90089-0740*

CAI PUIGDEFÀBREGAS *Servei Geològic de Catalunya, Avenida Paral·lel 71, 08004 Barcelona, Spain*

JOSEP ANTON MUÑOZ *Department de Geologia Dinàmica, Universitat de Barcelona, Zona Universitària de Pedralbes, 08071 Barcelona, Spain*

## ABSTRACT

Abundant and clearly exposed relationships between structures and syntectonic sedimentary rocks in the southern Pyrenees make this area particularly suitable for detailed studies of the sequential development of a collisional orogenic belt. During the Pyrenean orogeny, major shortening occurred in the eastern Pyrenees in Eocene and early Oligocene times. Until now, individual tectonic and depositional events have been only loosely defined temporally by biostratigraphic data. In order to provide a more precise chronological framework, four new magnetostratigraphic sections, spanning 8 km of Eocene strata and encompassing 18 m.y., have been developed in the eastern Pyrenees of northern Spain. The ages of nine major depositional sequences in the eastern Pyrenean foreland have been specified within the context of these chronologic data, beginning with the early Eocene transgression that commenced at 58 Ma. The timing of numerous tectonic events that occurred during the subsequent 16 m.y. can also be delineated, including the initial emplacement of the Pedraforca thrust sheet (58–54 Ma), the development of the Pedraforca breakback thrusts (47.5–40 Ma) at a mean shortening rate of 2.4 mm/yr, rotation of the Pedraforca footwall, three intervals of motion along the Vallfogona thrust (42.5–44.0, 40.5–41.5, and <40 Ma), creation of the Ripoll piggyback basin at 44 Ma, and the emplacement of the Ribes-Camprodon thrust sheet, beginning at ~42 Ma. Extensive evaporitic deposition, apparently coincident with sea-level lowering, occurred twice during Eocene times in the eastern Pyrenees: the Beuda sequence at ~49 Ma and the Cardona sequence at ~40 Ma. In response to continued tectonic encroachment on the northern margin of the foreland, the Eocene depocenter migrated southward ~80 km at a mean rate of 5 mm/yr, whereas indi-

vidual facies migrated at rates as high as 1 cm/yr. In the context of recent models of foreland basins, most of the major grain-size changes appear to be modulated by changes in subsidence rates, except in areas very close to active thrusts.

## INTRODUCTION

The goal of understanding the deformational and depositional history of a collisional mountain range can only be closely approached in special circumstances. Geologic structures must be clearly preserved in outcrop, as must related syntectonic strata. Exposures must be sufficiently extensive to provide a broad window onto the regional geologic record, and there must have been enough uplift and dissection to expose the main structural elements of orogen. To yield the clearest reconstruction, however, erosion must be strongly limited in order to reveal the near-surface structures and related strata, rather than solely the deeper-seated roots of the range. Finally, the tectonic assemblage must be amenable to chronologic evaluation in order to provide a temporal context within which to examine the evolution of the orogen.

The Pyrenees of northern Spain (Fig. 1) meet these criteria and have several other characteristics that assist in the reconstruction of a detailed tectonic synthesis. First, the semi-arid climate across the southern flank of the range has yielded abundant, clear exposures. Second, the amount of convergence that produced the Pyrenean orogen during latest Mesozoic and Paleogene times was relatively limited (~150 km; Muñoz, 1992). Many deformational events involved only a few kilometers of shortening, such that numerous structures are juxtaposed with the syntectonic strata that record much of their deformational history. Although major convergence was completed by Oligocene times, uplift and erosion of the orogen appears to have accelerated only during Plio-Pleistocene times. This circumstance has revealed detailed geometric re-

lationships between structures and syntectonic strata that are of a quality rarely described in other mountain chains. Finally, although the absence of volcanic strata renders many radiometric techniques inapplicable, high-quality temporal control can be achieved through a combination of biostratigraphic and magnetostratigraphic data.

This paper focuses on the chronology of deposition and tectonism in the eastern Pyrenees. New paleomagnetic studies provide closer temporal limits than previously attained and yield new insights on thrusting, rotational, and subsidence histories of this region.

## GEOLOGIC SETTING

During the Mesozoic and Cenozoic eras, the Pyrenean region of northern Iberia experienced a complex sequence of deformation in response to the opening of the Atlantic Ocean, closure of the Tethyan seaway, and both shearing and collision between the Iberian peninsula and southwestern Europe (Masson and Miles, 1984; Puigdefàbregas and Souquet, 1986; Muñoz, 1992). Although significant contraction began in late Cretaceous times with the development of the Boixols and related thrusts (Fig. 1) in the central Pyrenees (Simo, 1986; Berastegui and others, 1990) and with coeval thrusting in the Pedraforca area to the east (Vergés and Martínez, 1988), major shortening continued during Eocene time and culminated in late Eocene to early Oligocene times in the eastern Pyrenees.

Recent studies in the eastern Pyrenees (Muñoz, 1985; Muñoz and others, 1986; Puigdefàbregas and others, 1986; Martínez and others, 1988) have attempted to link the stratigraphic and structural records in order to develop a better understanding of Pyrenean deformation during Paleogene times. At a regional scale, successive emplacement of the upper (Pedraforca) and lower (Cadí) thrust sheets (Fig. 2), followed by growth of the basement-involved Freser Valley antiformal stack, out-of-sequence thrusting,

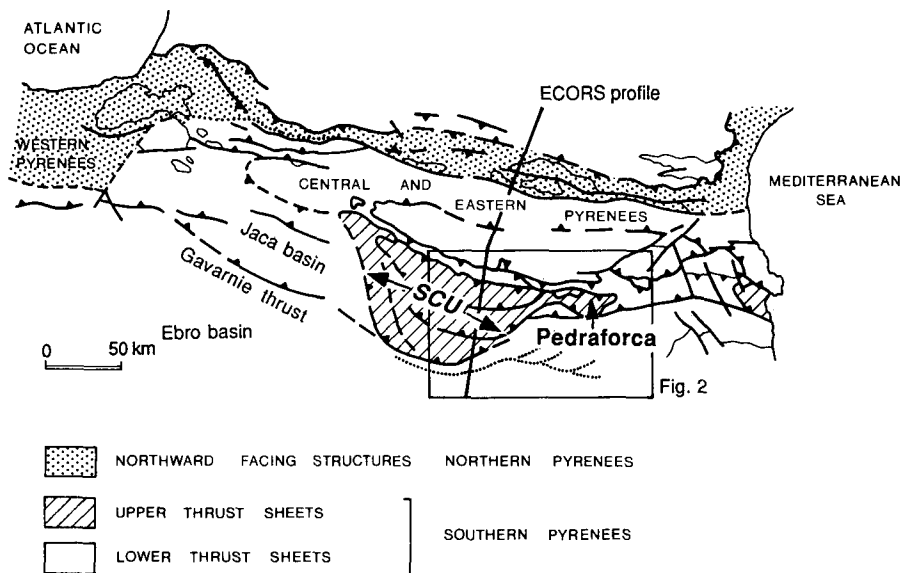


**Figure 1. General geologic map of the Pyrenees depicting Tertiary fold-and-thrust belts disposed along the flanks of the Axial Zone. Location of ECORS deep seismic profile is shown. SCU: South-Central Unit. Box indicates region covered by Figure 2.**

and development of frontal structures in the foreland (Vallfogona thrust) have been interpreted (Puigdefàbregas and others, 1986) as controlling nine large-scale depositional sequences in the eastern Pyrenean foreland basin (Fig. 3). Detailed mapping of parts of the Pedraforca allochthon has revealed clear cross-cutting relationships among individual thrusts and syntectonic strata (Fig. 4) that serve to document the development of coeval hindward-imbricating and piggyback thrusting (Martínez and others, 1988).

Until now, the chronology of the Eocene deformation in the eastern Pyrenees has been based on biostratigraphic data. The resolution attainable using the marine record is limited by the length of biostratigraphic stages (~1–3 m.y.) and by the unresolved overlap between stages as presently defined (Harland and others, 1990; Berggren and others, 1985; Aubry, 1985). In the terrestrial strata, the overall paucity of fossils and the imprecise ages inferred from them render their time resolution even less precise than that derived from marine strata.

Several problems result from this absence of detailed temporal control. Stratigraphic correlations between deposits in diverse geographic settings within the foreland basin usually cannot be made with a resolution better than several million years. The precise timing of deformational events cannot be specified, and many questions concerning synchrony or rates of tectonic and related depositional processes cannot be addressed in detail.

To resolve these problems, magnetic polarity stratigraphy has been utilized in several key localities in the foreland basin of the eastern Pyrenees to provide a detailed, correlatable chronologic framework within which to examine the diversity of tectonic and stratigraphic events in this region. The improved time resolution also serves to reveal the presence and duration of gaps in the depositional record and to identify discrete intervals of deformation. Here, we present the results of our magnetostratigraphic studies and discuss their implications for the evolution of the eastern Pyrenean thrust belt and adjacent foreland basin.

**METHODS**

Magnetic polarity stratigraphy was utilized in four related sections that encompass ~8 km of strata and include a total of 300 magnetic sampling sites (~1,100 specimens). Three sections are located within the Cadí thrust sheet and adjacent to the Pedraforca thrust sheet (Fig. 2). A fourth section (Vic) is located in the foreland, ~20 km south of the Vallfogona thrust. All sections include both marine and terrestrial strata and were measured using an Abney level and Jacob's staff. Sites were recorded on aerial photographs or on 1:5,000 topographic maps.

For each section, 10–12 triplets of specimens representative of various rock types found within the stratigraphic range of the section were selected for pilot demagnetization studies. Two specimens from each pilot sample level were

subjected to stepwise thermal demagnetization in ~50 °C steps, whereas a third was subjected to alternating-field demagnetization. The full complexity of the results of these pilot studies are beyond the scope of this paper, and only the salient points are summarized here.

The demagnetization behavior of the marine and terrestrial rocks was markedly different (Fig. 5). The sampled marine strata included marl, limestone, shale, and mudstone, whereas the terrestrial strata predominantly were overbank siltstone. Most marine specimens were weakly magnetized (typically 10<sup>-6</sup>–10<sup>-8</sup> emu/cc). An apparently modern overprint was typically removed by 240 °C (Fig. 5C–5F). Although some specimens with a reversed characteristic remanent magnetization (ChRM) did not fully lose this normal overprint until ~300 °C, all of the specimens with reversed ChRMs displayed their reversed polarity above 280 °C. Upon heating above 350–450 °C, many marine specimens, particularly marl and shale, exhibited much higher intensities, large increases in susceptibility, and inconsistent magnetic directions (Figs. 5D, 5F, 5I, and 5J). These changes appear to result from thermally induced oxidation of low Curie temperature magnetic minerals, particularly iron sulfides like greigite, that convert to magnetite during heating (Burbank and others, 1992).

Magnetizations due to iron sulfides tend to be weak and may be unstable. Because the iron sulfides are clearly post-depositional in origin, there is some question about whether they record the magnetic field near the time of deposition. In the eastern Pyrenees, we argue that we are recovering the original remanence directions based on the following observations: (a) polarities do not appear to be lithologically controlled; (b) lithologically identical, superposed sites may be oppositely polarized; (c) most magnetizations were acquired and stabilized prior to folding; (d) in lithologically similar rock units in the Esera and Isabena valleys (Powers, 1989), laterally separated, but demonstrably equivalent, marine strata reveal matching patterns of reversals; (e) discovered patterns of reversals can be matched with the magnetic time scale, with especially convincing matches in the most uninterrupted sections; and (f) nearly all reversals have been documented by multiple sites.

Whereas virtually all of the marine specimens were gray, most of the terrestrial strata were red, pink, or tan, due to variable pedogenesis. Although some terrestrial specimens exhibited large changes in susceptibility and became directionally unstable above 400–450 °C, many displayed a high coercivity, high-temperature stable remanence (Figs. 5A, 5B, 5G, and 5H). This

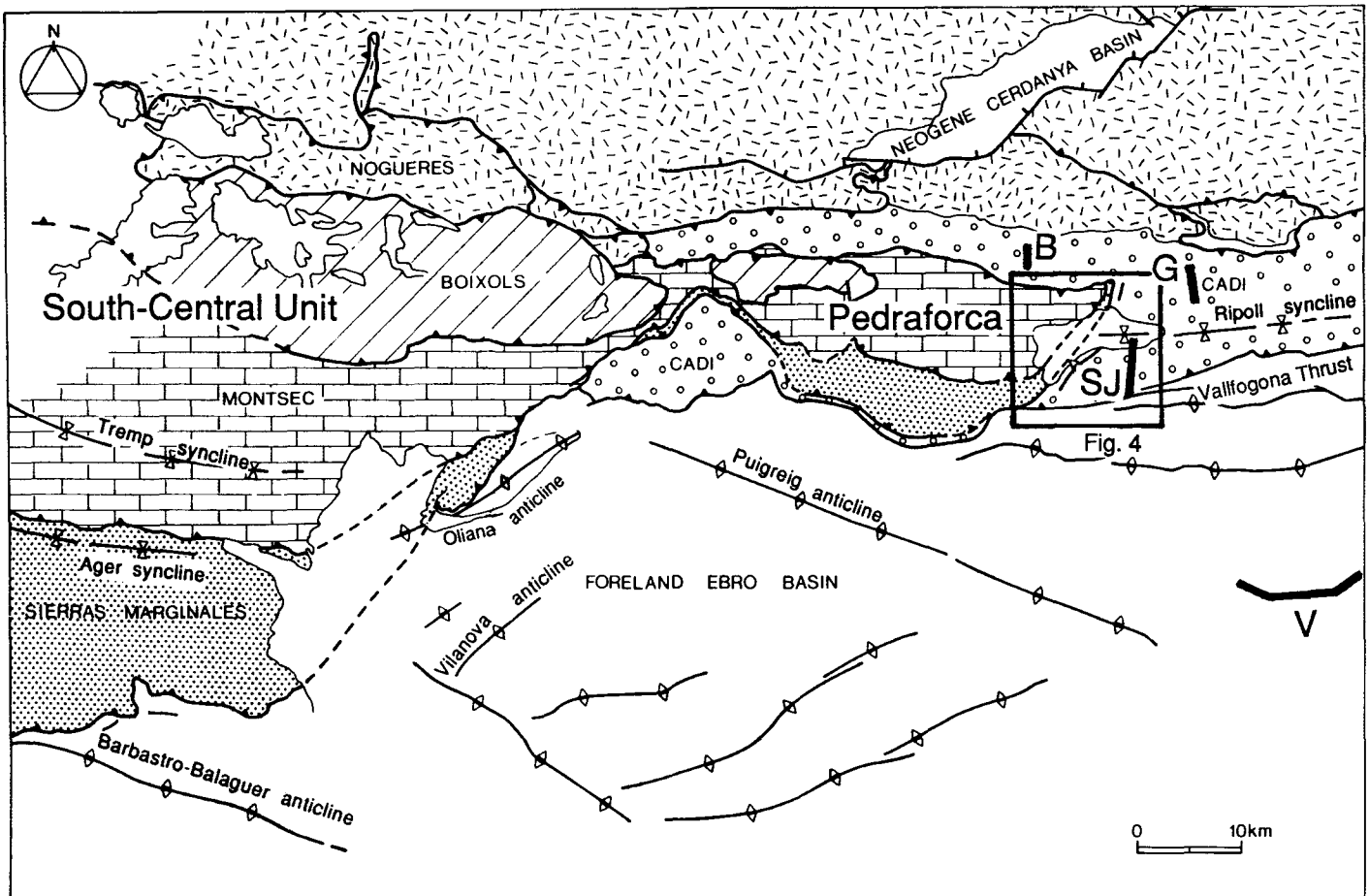


**Figure 2.** Simplified geological map of the eastern half of the South-Central Unit, the Pedraforca region that is the focus of this study, and the eastern extension of the Ebro foreland. Locations of magnetostratigraphic sections are indicated (B = Bagà; G = Gombren; SJ = St. Jaume; V = Vic). Box delineates the region shown in Figure 4.

component appears to reside in detrital hematite and probably also in authigenic hematite that formed during pedogenic reddening of these strata.

Given these demagnetization results, all remaining specimens were thermally demagnetized at 250, 280, 310, and 340 °C, and the ChRM was defined on the basis of these data. For sites in which mixed polarities were shown by individual specimens, additional heating steps up to 550 °C were applied. For those sites where this improved the clustering of the data, these higher temperature results were used to define the ChRM. The coherence of the data for each site was assessed using Fisher (1953) statistics. Sites were "Class I," if Fisher  $k \geq 10$ ; "Class II," if  $k < 10$ , but the site showed an unambiguous polarity; and "Class III," if the polarity was indeterminate. Class I data were used to calculate a mean rotation (if any) for each section. After removal of any vertical-axis rotation defined with respect to the Eocene magnetic pole

for Iberia, Class I and II sites were used to calculate the virtual geomagnetic pole (VGP) for each site. This VGP latitude was the basis for the local magnetic polarity stratigraphy (MPS). An  $\alpha_{95}$ -error envelope was calculated and plotted for each VGP latitude.

A fold test (McElhinny, 1964) based on the statistical grouping of directions before (*in situ*) and after corrections to restore the beds to horizontal (Table 1) is typically used to evaluate the possible presence of a post-tectonic magnetization. Due to either low (for example, Vic) or very uniform (for example, St. Jaume) dips throughout section, the improvement in clustering for the Pyrenean data after unfolding was not always statistically significant. It was more useful to assess whether the demagnetized directions appeared antipodal and whether either the *in situ* or corrected data yielded reasonable magnetic directions. For example, although the St. Jaume data do not pass the fold test (Fig. 6; Table 1), the *in situ* inclinations are nearly verti-

cal, whereas the corrected directions are inclined  $\sim 40^\circ$ – $50^\circ$ , as would be expected for Eocene times. Similar observations can be made in each of the other sections (Fig. 6A–6C), with the exceptions of (1) some of the normally magnetized data from Bagà (Fig. 6B), in which the *in situ* inclinations approach the modern dipole-field inclination ( $59^\circ$ ), whereas the corrected directions are nearly vertical, and (2) some normally polarized data low in the St. Jaume section, where fold-corrected inclinations are subhorizontal, whereas *in situ* ones approximate those of the present-day field. These sites at Bagà and St. Jaume apparently reflect a post-folding overprint and were not used in the local magnetostratigraphy.

In order to reconstruct sediment accumulation, the sections were decompacted using the method of Sclater and Christie (1980). Paleobathymetric estimates were made based on rock types and their enclosed faunas. These were combined with decompacted stratal thicknesses

S - N

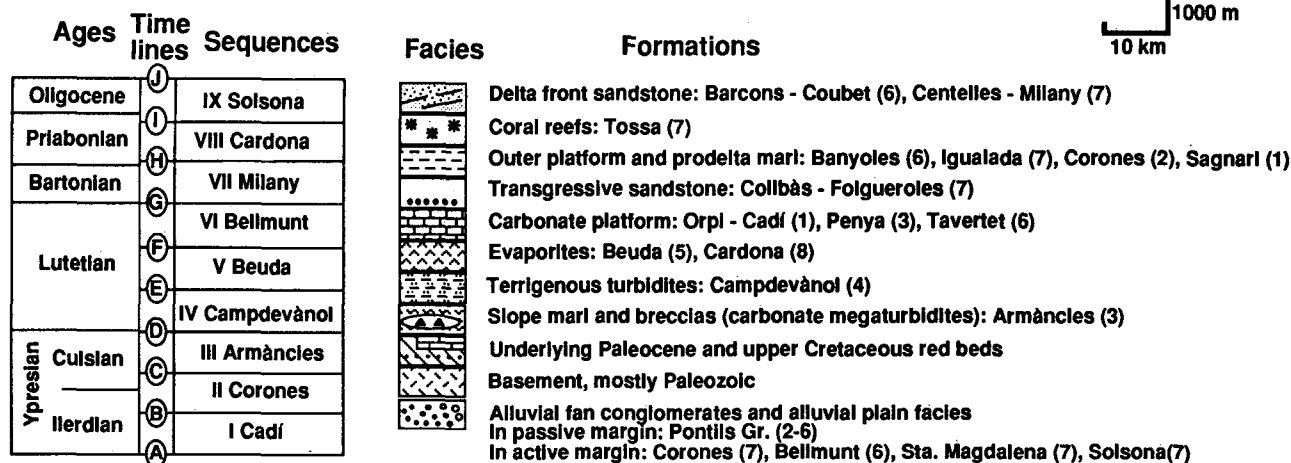
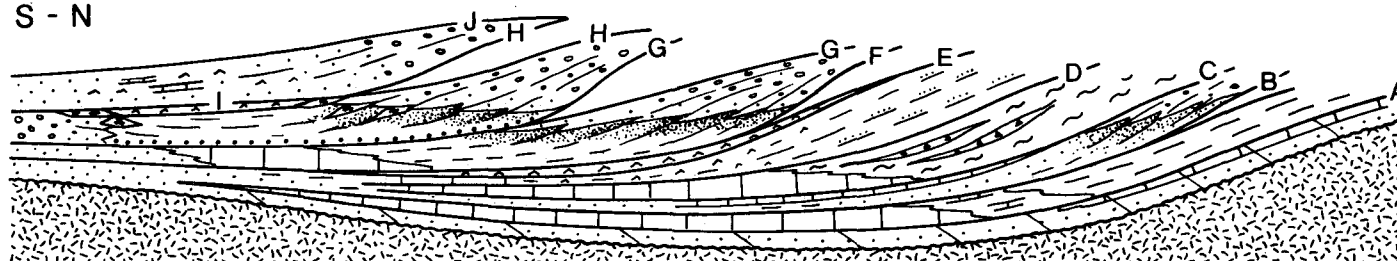


Figure 3. Idealized north-south cross section of the Eocene and lower Oligocene foreland-basin strata in the study area. Nine major depositional sequences, bounded by heavy, lettered lines, and their constituent sedimentary facies are schematically represented. The biostratigraphically and magnetostratigraphically defined positions of the sequence boundaries are depicted in the accompanying chart. (Modified from Puigdefàbregas and others, 1986).

to generate subsidence histories for each section. Although basement subsidence was calculated following conventional approaches (Sclater and Christie, 1980; Steckler and Watts, 1978; Guidish and others, 1985), tectonic subsidence was calculated at each step as the vertical difference between (1) the reconstructed position of the base of the decompact sediment column and (2) the position that that column would have if local Airy isostasy prevailed and there were no tectonic loads. This approach replaces "water-loaded" basement depths (Sclater and Christie, 1980) with a direct estimate of tectonic loading. Due to uncertainties in the subsidence curves arising from poorly known porosity, paleobathymetry, and cementation history, only large-scale changes in subsidence trends should be considered significant.

**RESULTS**

**Vic.** The Vic section is in the southeast to medial part of the Ebro foreland (Fig. 2). The basal part crops out within a few kilometers of exposed basement in the Catalan Coastal Range. The 1,300-m-thick section commences at the

top of the Taveret limestone (Figs. 7 and 8) and includes the Coll de Malla marls and the transgressive, glauconitic Folgueroles Formation. The remainder represents an upward-shallowing sequence of marl punctuated by southward-prograding sandstone tongues (for example, Oris sandstone) and succeeded by the St. Martí Xic deltaic complex, in which small reefs cap prograding sandstone lobes. The section ends in the

terrestrial Artés Formation, which unconformably overlies the Cardona evaporites farther to the south (Fig. 3). The Vic section thus spans the Bellmunt, Milany, and Cardona sequences, and the base of the Solsona sequence (Fig. 3; Puigdefàbregas and others, 1986).

Following demagnetization of the 72 sites, 32 (44%) were Class I, 14 (20%) were Class II, and 26 (36%) were Class III. Despite low and gener-

TABLE 1. FISHER STATISTICS ON MAGNETIC DATA

Section	Polarity	Number	<i>In situ</i>				Bedding corrected*			
			k	$\alpha_{95}(\circ)$	Dec. ( $\circ$ )	Inc. ( $\circ$ )	k	$\alpha_{95}$	Dec. ( $\circ$ )	Inc. ( $\circ$ )
Vic	N	60	5.7	8.6	359.6	43.1	7.8	7.4	358.4	45.2
	R	70	4.9	11.6	200.4	-43.4	10.1	7.7	201.1	-45.6
Bagà	N	34	7.4	9.9	355.7	48.2	7.3	9.9	251.6	81.9
	R	35	13.6	7.5	196.8	23.1	10.5	10.6	192.4	-32.9
Gombren	N	60	8.7	7.6	2.9	14.4	8.5	6.8	359.3	47.4
	R	64	3.2	12.0	155.1	39.9	7.7	8.2	165.9	-18.9
St. Jaume	N	74	18.7	3.7	3.8	76.2	17.8	4.1	353.7	39.6
	R	99	10.5	4.6	26.5	-79.7	14.1	4.4	165.5	-48.1
[52-50 Ma]†	N/R	65	9.5	5.5	22.3	78.8	15.1	5.5	344.3	47.5
[46-39 Ma]†	N/R	72	16.4	4.0	6.3	76.8	16.6	4.7	354.7	40.3

Note: k = Fisher's (1953) k;  $\alpha_{95}$  = 95% confidence interval on mean.  
 †These are combined normal and reversed data from St. Jaume for these intervals; reversed data are inverted.  
 \*Bedding correction assumes beds were horizontal at the time of deposition.

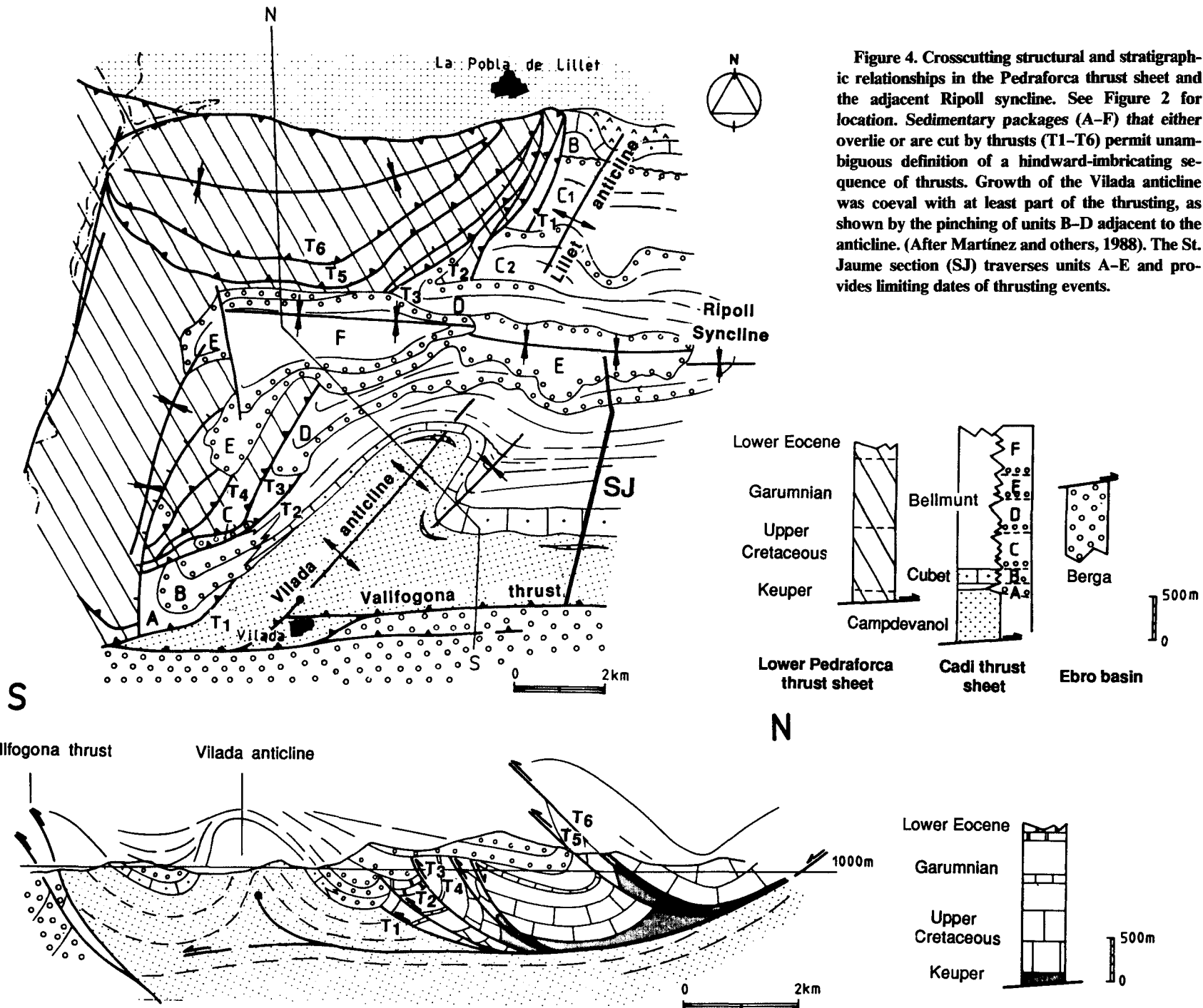
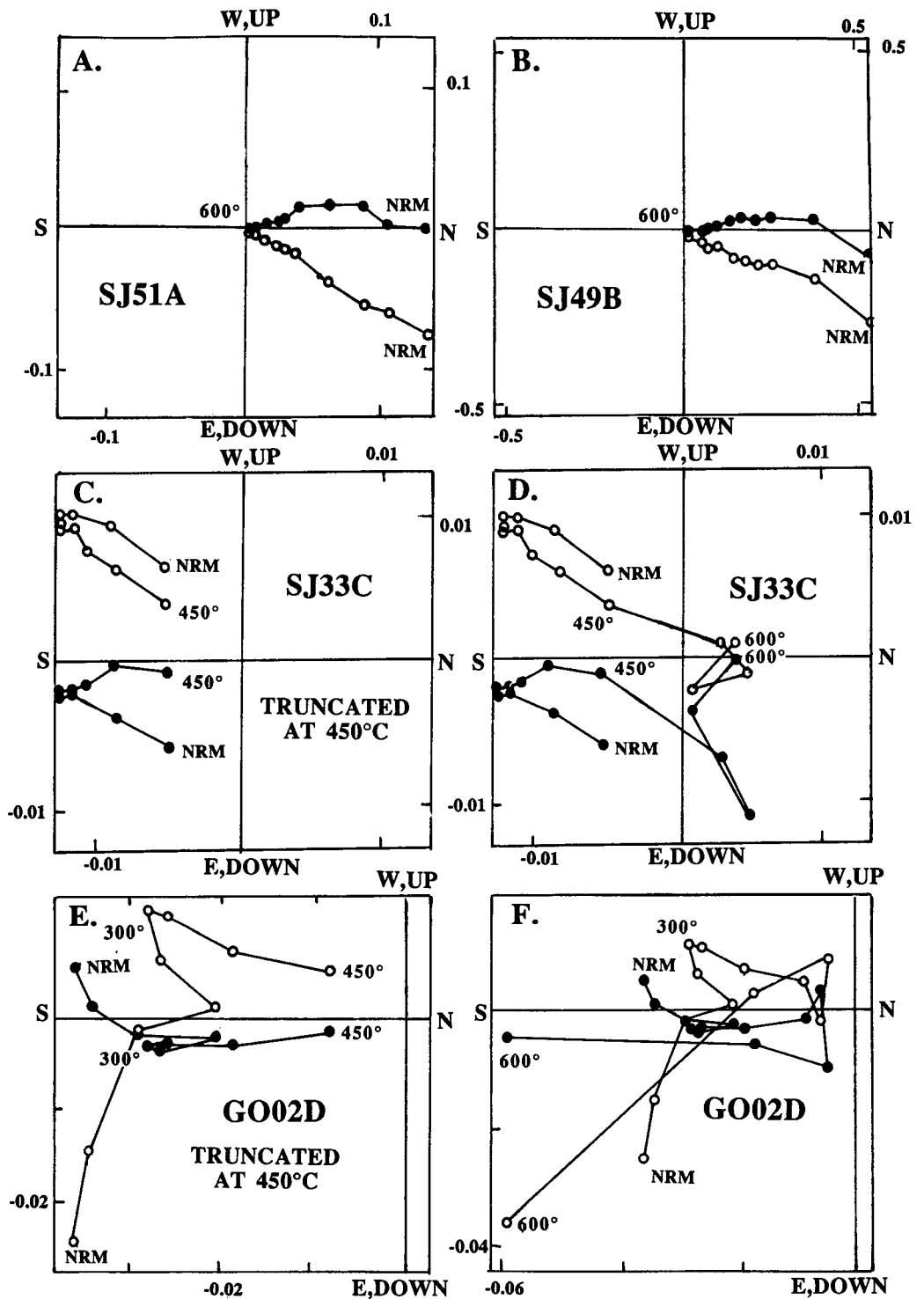


Figure 4. Crosscutting structural and stratigraphic relationships in the Pedraforca thrust sheet and the adjacent Ripoll syncline. See Figure 2 for location. Sedimentary packages (A-F) that either overlie or are cut by thrusts (T1-T6) permit unambiguous definition of a hindward-imbricating sequence of thrusts. Growth of the Vilada anticline was coeval with at least part of the thrusting, as shown by the pinching of units B-D adjacent to the anticline. (After Martínez and others, 1988). The St. Jaume section (SJ) traverses units A-E and provides limiting dates of thrusting events.

**Figure 5. Thermal demagnetization plots for representative specimens. Filled circles: declinations in the horizontal plane; open circles: inclinations in the vertical plane. A. SJ51A: normally magnetized terrestrial siltstone. Specimen shows largely single-component decay during demagnetization. B. SJ49C: normally magnetized terrestrial, slightly sandy siltstone, also normally magnetized. C. SJ33C: weakly magnetized, marine dark shale. Normal overprint is removed by 200 °C, and characteristic remanence is displayed between 200 and 400 °C. Truncated at 450 °C. D. Same as previous specimen, except erratic behavior at temperatures >450 °C is shown. E. GO02D: weakly magnetized marine marl. Easterly and downwards inclined overprint removed below 250–300 °C, characteristic remanence displayed above 250 °C, and truncated at 450 °C. F. GO02D. Same as previous specimen, except large intensity changes and erratic directions displayed above 450 °C. G–J. Intensity versus temperature plots for specimens shown at left. Note overprint removal below 250 °C for reversely magnetized specimens, and intensity increases due to oxidation above 450 to 500 °C.**



ally consistent dips, the Class I and II data pass fold and reversal tests and exhibit ~12° of clockwise tectonic rotation with respect to the expected Eocene direction (Fig. 6 and Table 1). This rotation is consistent with that found by

Parés and others (1988) in this region. The Vic MPS contains 15 magnetozones (Fig. 8), most of which are defined by multiple, superposed sites. Faunal data indicate that the top of the Tavertet limestone is of late Lutetian age (Regu-

ant, 1967), whereas the remainder of the section spans Bartonian and part of Priabonian times (Ferrer, 1971; Gich, 1972). The Artés Formation at the top of the section directly post-dates the Cardona evaporite (Sáez and others, 1991),

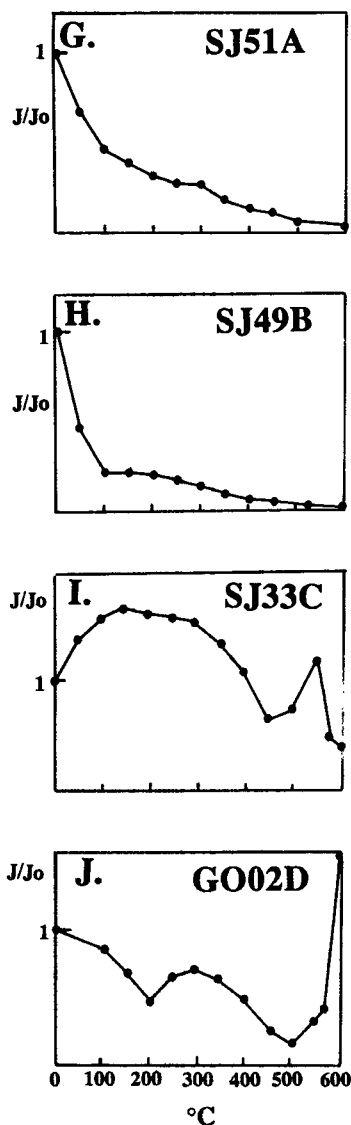


Figure 5. (Continued).

which itself is predicted to represent <100 ky (J. J. Pueyo, 1991, personal commun.). About 60 km to the west of Vic, the Cardona evaporite has a magnetostratigraphically defined date of ~40.0 Ma (Burbank and others, 1992). Given the faunal control and the dated tie point of the Cardona sequence, the Vic MPS can be correlated with the magnetic polarity time scale (MPTS; Fig. 9). This correlation indicates that the section spans from the top of chron 20 to the base of chron 16, an interval of ~6 m.y. (Berggren and others, 1985). Although the Vic MPS could be correlated with the MPTS in several different ways, the correlation shown here yields the smoothest (post-Folgueroles Forma-

tion) sediment accumulation and subsidence curve (Fig. 10) and is most consistent with the reversal pattern, with the available faunal age limits, and with the age of the top of the marine sequence. Because N2 and R2 are defined by single sites, it is possible that N1 represents chron 19 and that N2 is a transitional site at the base of chron 20. This would modify our interpretations only slightly.

**Bagà.** The Bagà section is located in the hanging wall of the Vallfogona thrust between the basement antiformal stack to the north and the outcrop of the Pedraforca thrust sheet to the south (Fig. 2). Beginning above Paleogene red beds, the section traverses the Cadí and Coronas sequences (Fig. 3). The Sagnari marls in the Cadí sequence appear to represent a rapid deepening during the initial stages of thrusting in the eastern Pyrenees (Pujadas and others, 1989). During this shortening, earliest Eocene extensional faults were inverted and overtopped by southward-prograding red beds in the upper Coronas sequence. A 700-m-thick section was sampled at 33 sites along the Bagà River (Fig. 11). Following demagnetization, twenty-one (64%) of the sites were Class I, six (18%) were Class II, and six (18%) were Class III. The demagnetized reversed data indicate ~20° of postdepositional clockwise rotation for this section (Fig. 6). Due to the previously described overprinting of some normal polarity sites, those sites yielding low VGP latitudes and large latitudinal errors were not included in the Bagà MPS.

The Bagà MPS contains five magnetozones and is dominated by >500 m of reversely magnetized strata (Fig. 12). Because the basal Cadí sequence is early Ypresian in age (Mey and others, 1968; Ferrer, 1971; Gich, 1972), the 500-m-thick reversed interval at the base of the MPS can be correlated with chron 24R (Fig. 9) that extends from ~56.0 Ma to 58.5 Ma (Berggren and others, 1985). Magnetozones N1–N2 could represent either chron 24 or both chron 24 and 23. Given the long reversely magnetized sequence that overlies the Coronas beds (see following section), we prefer to correlate the upper Coronas sequence with chrons 23 and 24. In this case, the top of the Bagà section dates from ~53.8 Ma, and the shelfal strata and red beds in the upper Coronas sequence exhibit very low net accumulation rates.

**Gombren.** The Gombren section is located along the northern limb of the Ripoll Syncline ~20 km east of Bagà (Fig. 2). The 3,000-m-thick section (Figs. 13 and 14) spans the Armàncies to Bellmunt sequences (Fig. 3) and

records a transition from marine to terrestrial deposition. The Armàncies sequence consists of slope marls, includes six limestone clast-bearing megaturbidites near its base, and is succeeded by siliclastic turbidites of the Campdevàdol Formation. The abrupt contact with the underlying marl suggests that an unconformity occurs at this contact. No angular discordance, however, was observed. Weak and unstable magnetizations found in many specimens led to a high proportion (40%) of Class III sites. Evaporitic deposition and probable constriction of the basin are indicated by the gypsum of the Beuda sequence, which is followed by transitional (Coubet) and then wholly terrestrial (Bellmunt) strata (Fig. 14).

Of the 94 magnetic sites, 39 (42%) are Class I, and 17 (18%) are Class II. The demagnetized data pass reversal and fold tests and exhibit negligible rotation. The Gombren MPS (Fig. 14) contains eight magnetozones, of which one (R2) is based on a single site. The correlation of the Gombren MPS with the MPTS (Fig. 9) is based on the Lutetian age of the Bellmunt sequence (Puigdefàbregas and others, 1986), on the middle to late Cuisian age of the megaturbidites in the Armàncies strata (Estevez, 1973; Puigdefàbregas and others, 1986; J. Serra-Kiel, 1990, personal commun.), and on the ages assigned to the Coronas strata on the basis of the Bagà magnetic section. The lateral separation (~20 km) between the Gombren and Bagà sections (Fig. 2), however, could permit considerable differences to occur in the age of the Coronas–Armàncies contact. Given that the stratigraphic separation of Armàncies megaturbidites above the formational contact remains nearly the same despite the distance between the two sections, it appears that the contact is only minimally time transgressive. The MPS correlation (Fig. 9) indicates that the Gombren section spans from the top of chron 23 (53.8 Ma) to the base of chron 20N (~46.0 Ma): an interval of ~8 m.y. The likely unconformity at the base of the Campdevàdol sequence is interpreted to be of brief duration.

**St. Jaume.** The St. Jaume section is located in the southern limb of the Ripoll syncline ~10 km southwest of the Gombren section (Figs. 2 and 15). The 3,100-m-thick section is delimited at its base by the Vallfogona thrust, which carries the Campdevàdol sequence in its hanging wall at this site. Like the Gombren section, the St. Jaume section includes the Beuda to Bellmunt sequences. It spans the entire Bellmunt succession, however, and includes both the Milany sequence and the Banyoles Formation (Rios

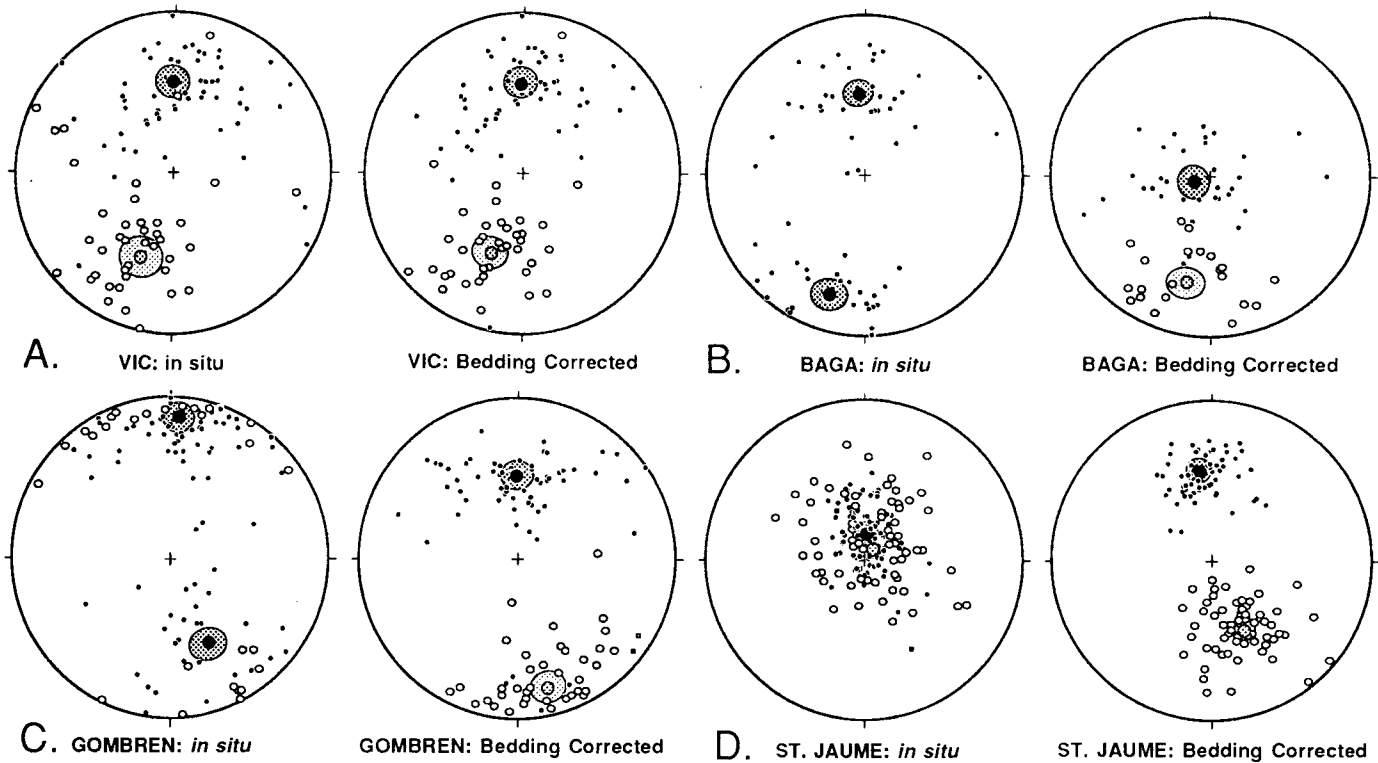


**Figure 6.** Equal-area stereonet plots of the demagnetized Class I data from the four studied sections. *In situ* and bedding-corrected directions are shown for each data set. Closed circles: lower hemisphere; open circles: upper hemisphere. Shaded ellipses represent 95% confidence cones on the mean directions. The St. Jaume and Gombren data are moderately to slightly rotated counterclockwise, and the Baga and Vic sections are similarly rotated clockwise. The statistical data related to each section are shown in Table 1.

and Masachs, 1953), a prodelta marine lithofacies not found in the more northerly Gombren section. A thin zone of terrestrial red beds is associated with the gypsum beds of the Beuda sequence. Granitic clasts first appear at ~2,400 m in the section and become increasingly abundant above this. Their appearance defines the base of the Milany sequence. These clasts have been interpreted as the denudation products from uplift of Axial Zone crystalline rocks (Fig. 1) due to large-scale out-of-sequence thrusting (Puigdefàbregas and others, 1986). The St. Jaume section also spans most of the syntectonic sequence (Fig. 4) that was deposited during the imbrication of the Pedraforca allochthon (Martínez and others, 1988). Whereas the most profound unconformities generated by this imbrication are located farther west, these unconformity-bounded packets can be traced into the sampled section. Hence, the dates from the magnetic section provide ages for the movement of individual thrusts. A major unconformity occurs at the top of the Bellmunt sequence, and stratal geometries (Fig. 15) within the syncline, as well as faulting of Bellmunt strata by the Vallfogona fault along the southern limit of the Ripoll syncline, suggest the uncon-

formity resulted from initial folding of the syncline about an east-west axis. Major paleocurrent changes occur within the St. Jaume section (Fig. 16); whereas the older strata indicate flow to the west and southwest, younger ones exhibit flow to the east and southeast.

Of the 93 magnetic sites in the St. Jaume section (Fig. 16), 53 (57%) were Class I, 18 (19%) were Class II, 14 (15%) were Class III, and 8 (9%) appeared to be overprinted. Stereoplots of the Class I data (Fig. 6D) indicate that they pass the reversal test and that they have undergone a syndepositional, differential rotation. The pre-Beuda strata are rotated counterclockwise ~15°, whereas the younger Bellmunt and Milany strata are only rotated ~5° (Table 1). Due to nearly uniform dips throughout the section, the fold test is not statistically significant. The *in situ* directions, however, appear to have no geologic meaning, whereas the unfolded directions provide reasonable Eocene polarities (Burbank and Puigdefàbregas, 1985). Eight sites (x's, Fig. 16) between 150 and 375 m appear to exhibit normal polarity. Their *in situ* inclinations, however, are similar to that of the modern field, and their bedding-corrected inclinations are subhorizontal. We interpret these sites to

contain a modern overprint that thermal demagnetization failed to remove. These sites, therefore, are not included in the MPS for the St. Jaume section.

The St. Jaume MPS (Fig. 16) contains eight magnetozones, of which one (N2) is based on a single site. The correlation of the St. Jaume MPS with the MPTS (Fig. 9) is assisted by faunal and stratigraphic data. First, nannoplankton from the Campdevànol turbidites (Van Eeckhout, 1990) indicate that the transition between zones NP14 and NP15 occurs below the Beuda sequence. According to Aubry (1985) and Berggren and others (1985), this transition occurs at ~50 Ma near the base of chron 21N. Second, abundant Bartonian fossils have been found directly above the unconformity at 2,075 m (Moya and others, 1991). Hence, this part of the section should be younger than ~44 Ma. Finally, mapping south of the Vallfogona thrust shows that the Bellmunt sequence is cut by early imbricates of the thrust and is overlain by the Folgueroles Formation. Our dates on the Folgueroles Formation from Vic (Figs. 8 and 9) thus indicate that Bellmunt deposition must have ceased before ~44 Ma.

Given these limits and the stratigraphic links

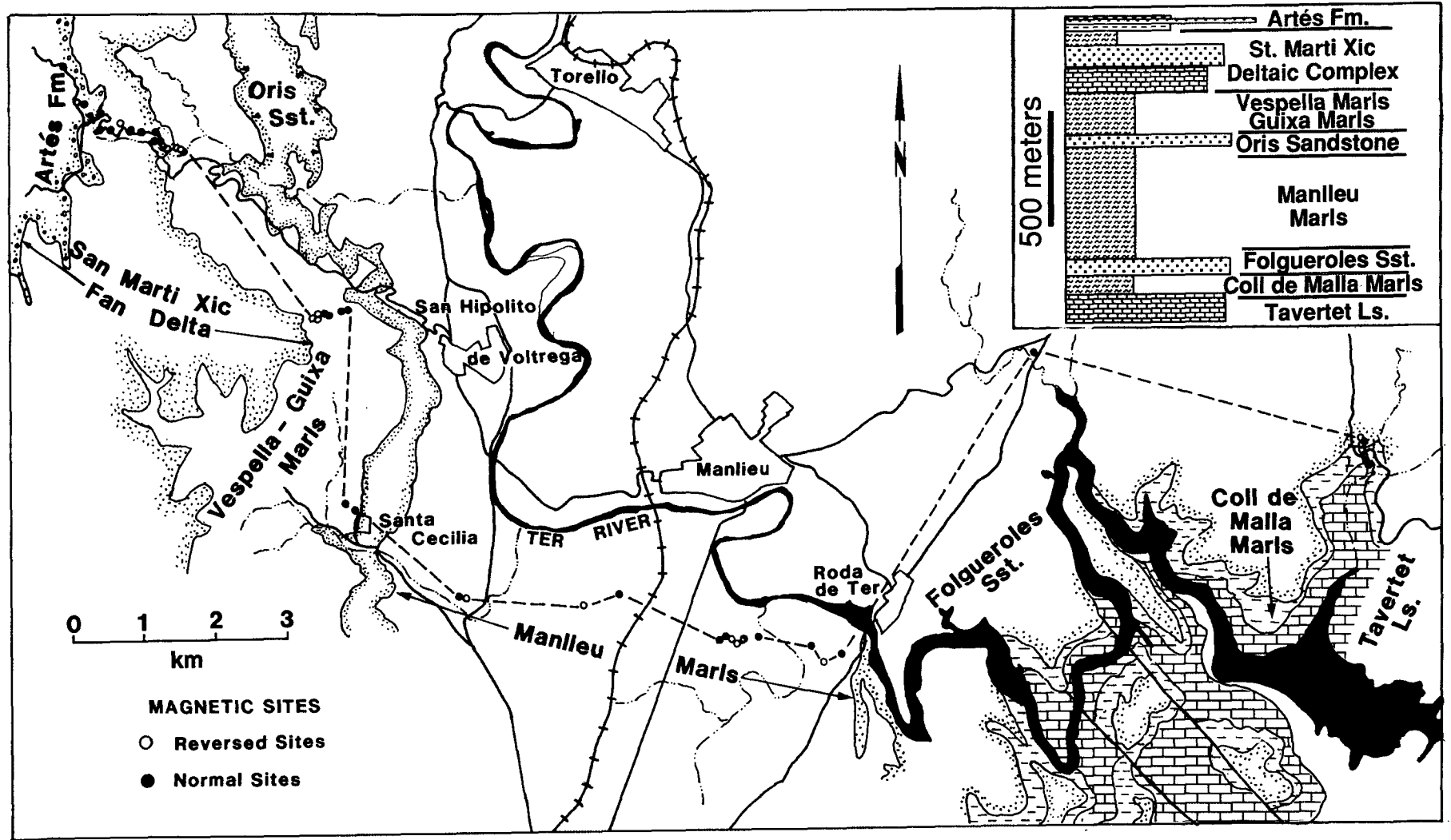
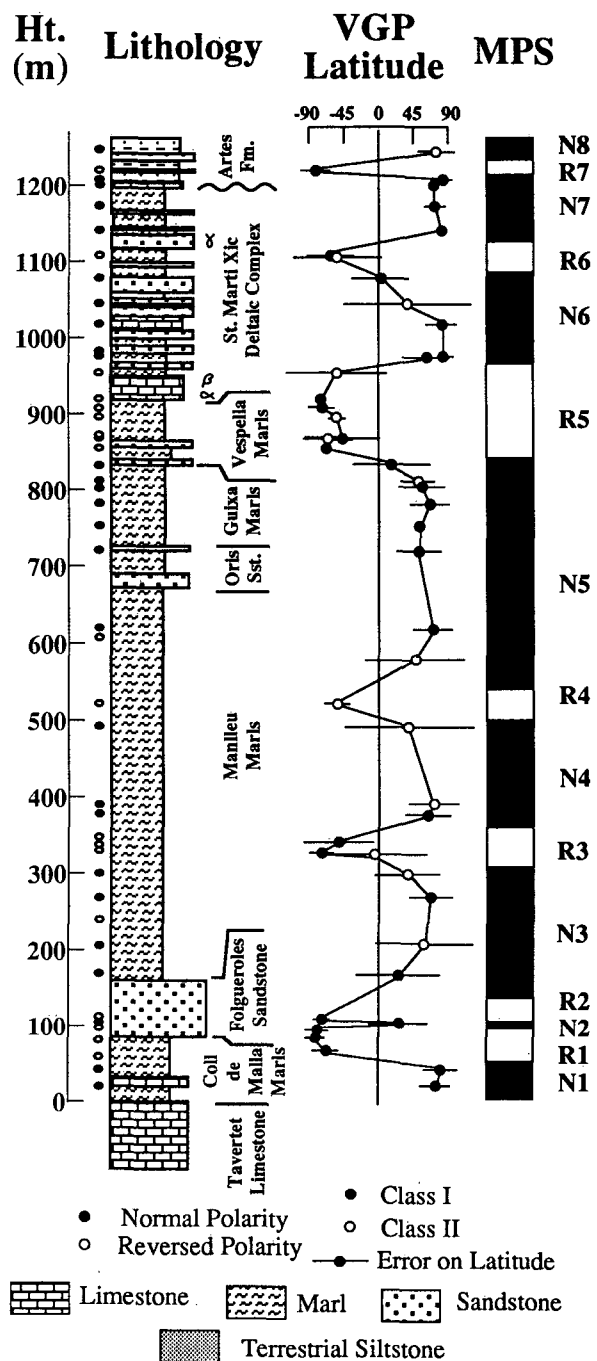


Figure 7. Location map for the Vic magnetic section. Large lateral extent of the magnetic traverse (shown by dashed line) is due to low relief and shallow dips of the upper Eocene strata. Inset shows the schematic stratigraphy of the Vic section. See Figure 2 for section location.

Figure 8. The Vic magnetic polarity stratigraphy (MPS). The stratigraphic height of Class I and II reversely (open circles) and normally (filled circles) magnetized samples are plotted adjacent to the simplified stratigraphic column within which the major formational boundaries are identified. Confidence limits ( $\alpha_{95}$ ) are plotted on the calculated latitude of each virtual geomagnetic pole (VGP). In the MPS, black bars denote normal polarity, white bars denote reversed polarity, and each of the magnetozones is sequentially numbered.



least a 1.2-m.y. gap centered at ~43 Ma. Between 52 Ma and 46 Ma, ~10°–15° of counter-clockwise rotation occurred.

DISCUSSION

Correlations with the Magnetic Time Scale

At present, the Eocene to Oligocene MPTS is undergoing revision. Chronologic data (Montanari and others, 1988; McIntosh, 1988) indicate that the Eocene/Oligocene boundary will be shifted 3–4 m.y. younger. A similar revision is also likely to occur in the early Eocene time scale (W. Berggren, 1990, personal commun.). Hence, it is likely that the ages quoted here will need revision to conform to an improved time scale. Because neither the overall duration of Eocene time nor the general pattern of reversals is expected to change significantly, the correlations of the local magnetozones to the MPTS and the rates calculated here should retain their overall validity.

The correlation of the local magnetic polarity stratigraphies with the MPTS (Fig. 9) is assisted by previously attained biostratigraphic data (Reguant, 1967; Ferrer, 1971; Estevez, 1973; Serra-Kiel, 1981; Orti and others, 1985). These data provide generalized "tie-points" of 1–4 m.y. duration between the local MPS and the MPTS. Because the Pyrenean biostratigraphy is based primarily on nummulites that have not been definitively tied to the northwestern European biostratigraphy (Aubry, 1985), uncertainties remain concerning the chronologic significance of the Pyrenean biostratigraphic data. Additional guides to correlation with the magnetic time scale are found when sedimentary formations interfinger at different localities, such that unambiguous dating of a formation at one locality serves to guide correlations with the MPTS at other localities. Finally, identified unconformities or intervals of slow sediment accumulation (for example, glauconitic sands) suggest stratigraphic intervals where breaks may occur in the local MPS.

Whereas the correlations shown in Figure 9 have been guided by the faunal, stratigraphic, and sedimentologic data described above, some ambiguities remain in the correlations. Our interpretations require the Beuda sequence at St. Jaume and the upper part of the Coronas sequence at Bagà (Fig. 9) to be highly condensed and to represent 1–2 m.y., whereas the unconformity between the Armàncies and Campdevànol strata at Gombren is interpreted to have lasted less than 0.1 m.y. These interpretations

to the nearby Gombren section, the St. Jaume MPS can be correlated to the MPTS from near the base of chron 21R to either chron 17 or 18 (Fig. 9). The unconformity at 2,075 m appears to represent a gap extending from the base of chron 18N to chron 19R. Whereas chron 21R encompasses the Campdevànol turbidites, chron 21N appears to be represented by the condensed section of Beuda evaporites and may contain an

unconformity at their base. The Bellmunt red beds begin at 46.2 (chron 21N), and the Milany red beds begin at ~42.7 Ma (chron 18N). The topmost sampled strata in the Milany sequence here could correlate to any part of chron 17 or 18, but if they were to correlate to chron 18, it would require very rapid sediment accumulation. Following this interpretation, the St. Jaume section spans from 51.9 Ma to ~40 Ma with at

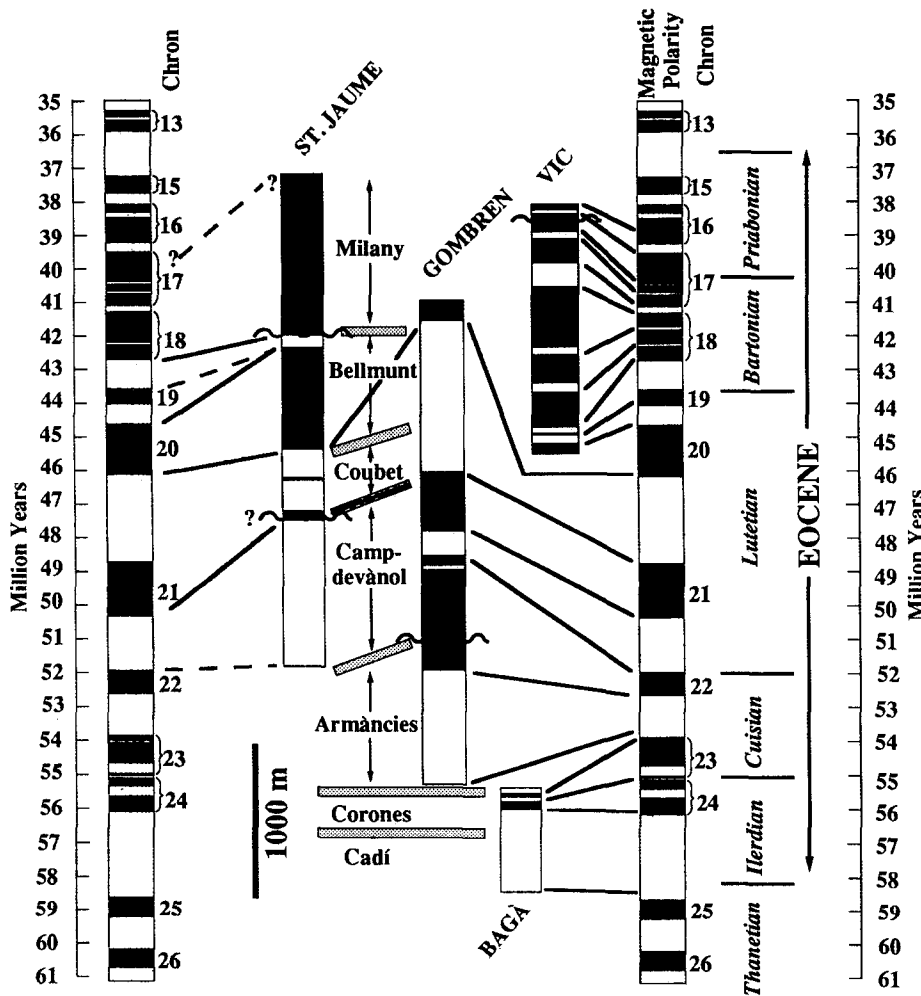


**Figure 9.** Correlation of each of the local MPS's from the eastern Pyrenees with the magnetic polarity time scale of Berggren and others (1985). Chron numbers (13–26) are adjacent to the normal magnetozones of each chron. The underlying, reversed magnetozones also belong to that chron. Stage names, boundary positions, and ages are also taken from Berggren and others (1985). The dot-filled boxes indicate the position and correlation of sequence boundaries between the St. Jaume and Gombren sections, whereas the heavy lines show the correlations we have defined between each of the local MPS's and the MPTs. The wavy lines indicate the position of unconformities within the studied sections, and dashed lines denote uncertain or alternative correlations. See text for a discussion of the choice of correlations, biostratigraphic controls that guided each correlation, and problems and implications of each correlation.

are a direct consequence of matching the reversal patterns of each section with the magnetic time scale, and they are based on the assumption that the time scale is well known. The duration of the hiatus identified in the St. Jaume section (2,100 m, Fig. 16) depends on whether the topmost normal magnetozones (N4) is correlated with magnetic anomaly 17, 18, or 19 (Fig. 9). The correlation we have chosen (to chron 17)

yields both a reasonable gap at the basal unconformity of the Milany sequence and subsidence rates that are rapid, but consistent with other sections (Fig. 10). Other correlations, however, cannot be eliminated with confidence.

The correlation of the base of the Vic section (Figs. 8 and 9) is also ambiguous. The topmost Tavertet Formation is of upper Lutetian age (Reguant, 1967), and magnetozones N1 could,

therefore, correlate with either anomaly 19 or 20. The Coll de Malla marl and the glauconitic sandstone of the Folgueroles Formation suggest slow deposition during this interval, such that the reversed interval (chron 19R) could be represented by the stratigraphically thin, reversed magnetozones (R2) in the middle of the Folgueroles at Vic. The topmost Tavertet would then correlate with anomaly 20. We prefer this interpretation, but can not eliminate the possibility that the Tavertet extends to anomaly 19.

Given the density of sampling, the discovered patterns of reversals, the observed unconformities within the sections, and the available biostratigraphic controls, there is little flexibility in the general correlations with the MPTs (Fig. 9). The proposed correlations of the detailed pattern of short-duration reversals within anomalies 17, 18, 23, and 24 (Fig. 9), however, may be modified in the future, if the sampling density, specimen quality, and stratigraphic resolution are increased.

#### Implications of the Chronologic Record

On the basis of these new magnetostratigraphic data, strata spanning an interval of 18 m.y. during Eocene time have been dated with a much higher resolution than previously attained. Because this interval encompasses a time of major shortening within the eastern Pyrenees, these data provide a precise temporal framework within which to analyze related tectonic and depositional events. The ages quoted below are derived from the time scale of Berggren and others (1985). Other relevant data, such as eustatic histories (Haq and others, 1987) or faunal records (for example, Aubry, 1985), which are cast in the context of the MPTs, are converted to absolute ages according to Berggren and others' (1985) time scale.

The oldest record studied here comes from the Bagà section located in the footwall of the Pedraforca thrust sheet (Fig. 2). The marl of the Sagnari Formation (Gich, 1972) and the Alveolina limestone (Mey and others, 1968) of the Cadi sequence began to accumulate here at ~58 Ma (Fig. 18), or in earliest Eocene time. These units overlie Paleocene terrestrial red beds and lacustrine limestones, and they appear to result from a widespread transgression that culminated during latest Thanetian to earliest Ilerdian times (Ypresian; Haq and others, 1987). Limestone of similar age is found over much of the central Pyrenees (Barnolas and others, 1991). East of the study area, the Sangari marl was deposited in a trough that apparently subsided rapidly due

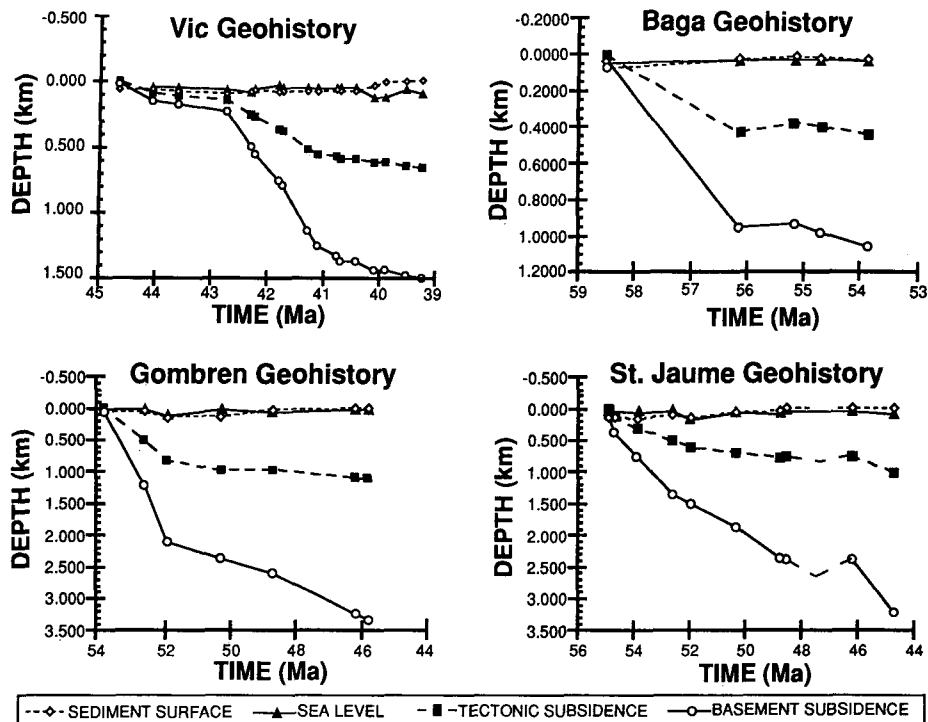


**Figure 10.** Geohistory curves for each of the dated sections. Decompacted thicknesses were calculated according to the algorithm of Sclater and Christie (1980). Paleobathymetry is estimated from faunal data, wherever possible, and sea level is referenced to the early Eocene high stand and represents departures from that level determined by Haq and others (1987). Basement depth is calculated as the sum of decompacted thicknesses, paleowater depths, and sea-level position. Tectonic subsidence is calculated as the difference between the calculated position of the basement assuming local Airy isostasy and the reconstructed ("observed") position of the basement as described above. Due to uncertainties in water depth, sea-level position, original porosity, and cementation history, an error of ~10% is likely to be associated with each estimate.

to loading by the Empordà thrust sheet (Pujadas and others, 1989). Hence, shortening and transgression in the eastern Pyrenees took place coevally at ~58 Ma.

Despite possibly being deposited during a relative high stand of sea level (Haq and others, 1987), the middle Coronas sequence at Bagà (Figs. 11 and 12) includes a northerly supplied deltaic system that is inferred to correlate with the basin inversion and southward-prograding red beds observable 30 km to the east (Pujadas and others, 1989). The net sediment accumulation rate is slow during this interval (5–9 cm/ky), and numerous small unconformities may have developed under a regime of minor tectonic uplift (Fig. 10).

Rapid deepening of the proximal foreland basin is recorded by the slope marl and breccias of the Armàncies sequence, which represent an abrupt change in the style of deposition, beginning at ~53.9 Ma within middle Cuisian times (Gombren section, north limb Ripoll syncline, Figs. 14 and 17). Decompacted sediment-

accumulation rates and subsidence accelerate at this time (80–100 cm/ky; Fig. 10). This deepening is viewed as a response primarily to loading by the Pedraforca thrust sheets and secondarily to the relatively high sea level during this interval (Haq and others, 1987). Megaturbidites (or slope breccias) up to 30 m thick in the lower parts of the Armàncies contain clasts of Iberian limestone within a matrix of middle to upper Cuisian age (Puigdefàbregas and others, 1986). The only presently known directional indicators in the megaturbidites suggest westerly flow. Because this direction is subparallel to the reconstructed basin axis (Puigdefàbregas and others, 1986), it remains unclear whether these megaturbidites had a northerly or southerly source. Although some of the megaturbidites exhibit sedimentological evidence for deposition from a single catastrophic event, others appear to record several superposed depositional events. Similar megaturbidites in the western Pyrenees have been interpreted as representing large seismic events (Séguret and others, 1984). Whereas

an analogous causal mechanism is likely for the eastern Pyrenees, the superimposition of several megaturbidites with no intervening fine-grained strata suggests that destabilization of the carbonate shelf (perhaps by minor sea-level lowering) often was a precursor to catastrophic collapse of the shelf margin during submarine thrusting. A similar temporal coincidence of pulses of tectonism with significant sea-level drops has been inferred to provide the necessary conditions for generating submarine breccias in several other localities (Garrison and Ramirez, 1989).

Along the northern limb of the Ripoll syncline, the Armàncies strata are overlain by the turbiditic Campdevàrol sequence, which attains a thickness of ~1 km (Fig. 14). Because the turbidites contain abundant macerated plant debris and are strikingly siliciclastic, they appear to be dominated by terrestrial source areas. In the Gombren section, turbidites appear abruptly at ~52.1 Ma and, according to our correlation with the MPTS (Fig. 9), accumulate at a mean rate of ~30–50 cm/ky until ~49.5 Ma. A distinct unconformity between the marl and the terrestrially sourced turbidites occurs within chron 22N (Figs. 9 and 12). According to Haq and others (1987), the largest sea-level drop and rise (>100 m) in Eocene times occurs here at the Cuisian-Lutetian boundary. The apparent brevity of this sea-level fluctuation, despite its magnitude, supports our contention that relatively little time (<0.2 m.y.) is represented by this unconformity.

On the southern limb of the Ripoll syncline in the St. Jaume section, Vallfogona thrust has truncated the Campdevàrol turbidites above their contact with the Armàncies sequence. These west-southwest-directed turbidites (Fig. 16) span an interval from 50.0 Ma to 51.9 Ma (Figs. 9 and 17). Their rate of decompacted sediment accumulation is calculated to be 70–80 cm/ky prior to ~50 Ma (Fig. 10). The subsidence rates during both Armàncies and Campdevàrol deposition display a significant acceleration over those during Coronas deposition (Fig. 10). We interpret this rapid deepening, as well as the presence of megaturbidites that were probably triggered by seismicity, as a response to thrust-induced subsidence and infer that emplacement of the Pedraforca allochthon occurred between 54 Ma and 50 Ma.

The end of turbiditic deposition is marked by decreasing subsidence rates (5–15 cm/ky; Fig. 10), by distinctive upward shallowing, and by the development of a red bed and evaporite sequence (Beuda Formation). Along both the northern and southern limbs of the Ripoll syncline, Beuda strata are ~48.7–49 Ma, or early Lutetian age (Figs. 14, 16, and 17). Eustatic reconstructions (Haq and others, 1987) indicate a

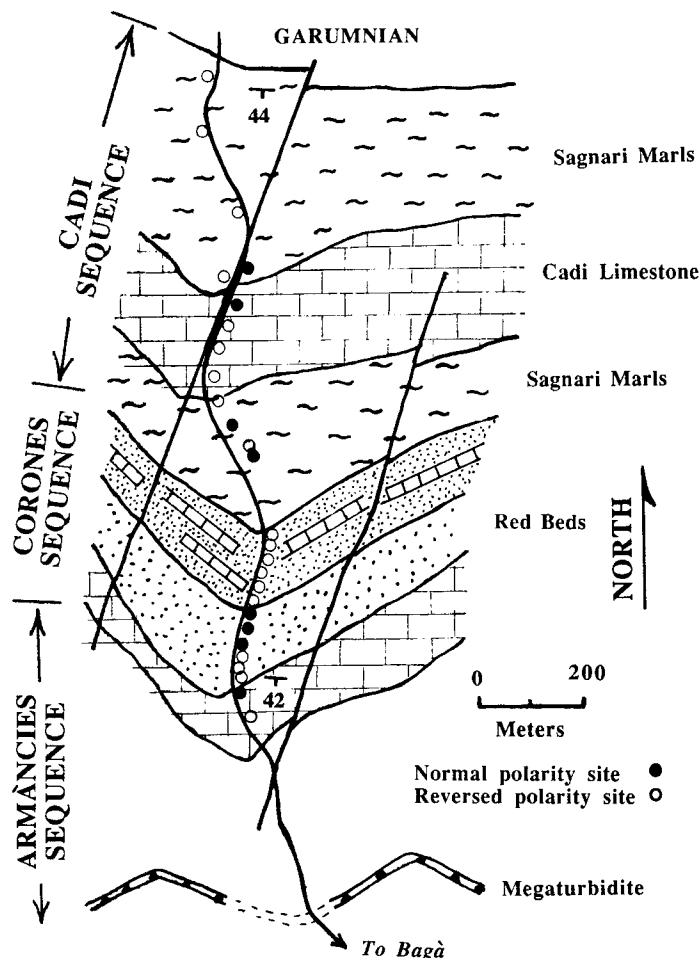


Figure 11. Location map for the Bagà section based on aerial photographs and 1:50,000 maps. See Figure 2 for section location.

sea-level fall (~50 m) at this time. Basin constriction may also be attributable to topographic damming by the oblique termination of the Pedraforca thrust sheet. Although this time has been cited as the end of the first stage of Pedraforca thrusting (Puigdefàbregas and others, 1986), we suggest that the decreasing subsidence rates may imply that the rate of erosion and removal of the thrust load began to exceed the rate of load emplacement (Flemings and Jordan, 1990), that the sediment supply decreased dramatically, and/or that thrusting stopped altogether at this time.

The prodelta and delta-front sandstone and shale of the Coubet Formation directly overlie the Beuda evaporite in the northern Ripoll syncline. On the southern limb, ~200 m of "blue shale" (Banyoles Formation) precedes the earliest Coubet strata. Both formations display renewed acceleration of sediment accumulation and subsidence (~20–50 cm/ky; Fig. 10), and in the south, the Banyoles strata indicate deep-

ing marine conditions. The Coubet strata mark the transition to predominantly terrestrial deposition in the northern parts of the foreland basin, and they are followed by the generally southward-prograding alluvial strata of the Bellmunt Formation. In the north, the Bellmunt red beds first appear at ~47.5 Ma (Fig. 17) and coarsen upward to the top of the presently preserved sequence, where abundant conglomerate beds are dated at ~45.8 Ma (Gombren section; Fig. 14). In the southern synclinal exposures, the Bellmunt strata first appear ~1–1.5 m.y. later than in the northern limb. This diachrony suggests southward progradation of the Bellmunt fan at a mean rate of 0.5–1.0 cm/yr. Within 300 m of the top of the Bellmunt sequence at St. Jaume, rare interbeds of nummulitic sandstone still appear. Their stratal geometries indicate that the basin remained open to the southwest at this time. Stratigraphic relationships still farther to the south near Vic (Fig. 2) indicate that the Tavertet Formation underlies the prograding

Bellmunt fan. Thus, by comparison with dated strata farther north, the Tavertet limestone may date from >46 Ma.

Although the clastic rocks that supersede the Beuda strata generally represent an interval of erosion of the Pedraforca thrust sheet (Puigdefàbregas and others, 1986), a hindward-imbricating fan of thrusts began to develop within the thrust sheet (Fig. 4) at this time (Martínez and others, 1988). Between 47.4 Ma and 40.0 Ma, four individual thrusts (T<sub>1</sub> to T<sub>4</sub>; Figs. 4 and 16) cut fan strata that can be correlated with the Banyoles to Milany strata at St. Jaume (Fig. 17). Due to the coarse-grained strata in the core of the Ripoll syncline, the youngest thrust could not be dated using paleomagnetic techniques. Breakback thrusting appears to be due to internal deformation of the Pedraforca thrust sheet during the development of the Ripoll syncline between the emergent frontal thrust to the south and the growing Freser Valley antiformal stack to the north (Muñoz and others, 1986).

Coeval with the start of breakback thrusting (T<sub>1</sub>) at ~47.4 Ma, piggyback thrusting led to initial development of the Vilada anticline (Figs. 4 and 17). Whereas early anticlinal growth was not rapid, accelerated growth of the anticline occurred between 46 Ma and 42 Ma. This disruption profoundly affected strata in the southern Ripoll syncline, causing thinning and stratal truncation adjacent to the anticline (Fig. 4). Anticlinal growth continued to deform syntectonic strata until 41 Ma, after which no younger strata appear disturbed by this fold.

Initial movement of the Vallfogona thrust occurred during growth of the Vilada anticline and breakback thrusting, as ~5 km of shortening disrupted the Bellmunt red beds prior to deposition of the Folgueroles Formation, transformed the Ripoll basin into a piggyback basin, and caused folding about an east-west axis. Between 44 Ma and 42.5 Ma, shortening averaged 3 mm/yr and created the unconformity that bounds the base of the Bartonian Milany strata at 2,075 m in the St. Jaume section (Figs. 16 and 17). Paleocurrents in the Milany sequence at St. Jaume (Fig. 16) and coeval stratal patterns in the northern Ripoll syncline (Martínez and others, 1988) indicate that transformation to a piggyback basin and continued development of the Pedraforca imbricates caused fans to prograde eastward into the newly formed syncline.

Two additional intervals of Vallfogona thrusting can be defined. During Milany deposition (42–40 Ma), Vallfogona imbricates cut the Folgueroles sandstone. Relative quiescence prevailed during deposition of the Cardona evaporite (~40 Ma), and an unconformity developed across the Vallfogona imbricate fan (Fig. 17). The overlying Berga conglomerates are correla-

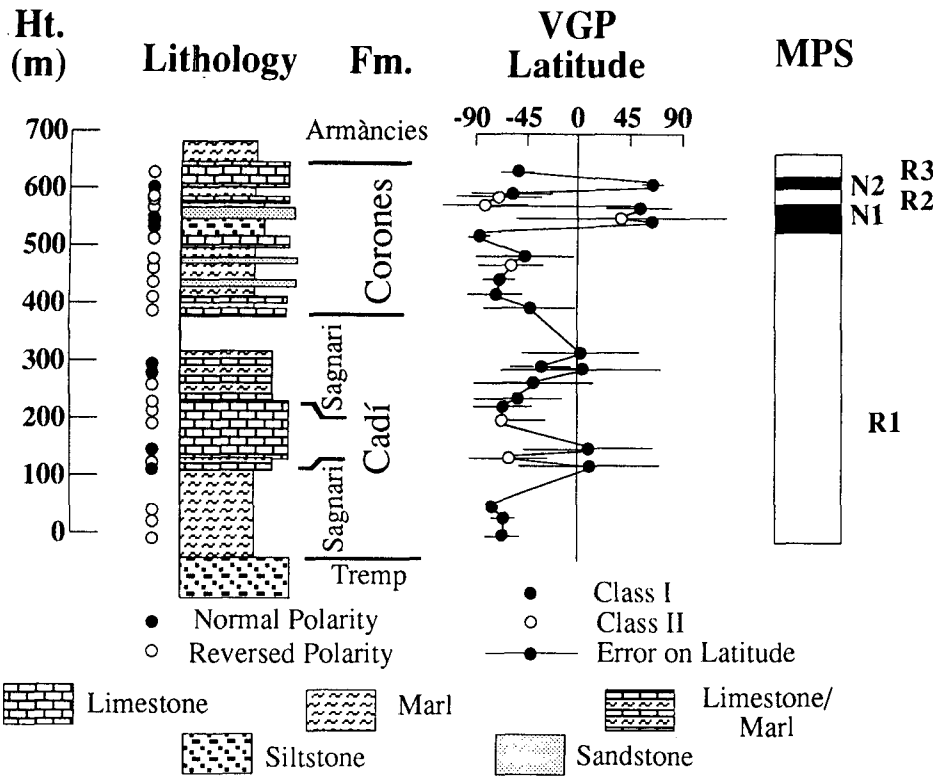


Figure 12. The Bagà MPS. Sites indicating normal polarity below 350 m appear to represent post-folding overprinting and were not included in the zonation of the MPS. For description of symbols, see Figure 8.

significant unconformities in proximal areas and were followed by intervals of slower shortening. In addition, two different scales of piggyback thrusting can be discerned. Limited shortening (~1 km) occurred within the Vilada anticline immediately adjacent and closely parallel to the breakback thrusts (Fig. 4). The thrust causing this shortening used the same sole thrust as was used by the breakback imbricates. In contrast, the Vallfogona piggyback thrust is a more regional feature that is oriented orthogonally to the primary, north-south transport direction. It utilized a deeper detachment surface, as it translated both the Ripoll basin and the imbricate stack into a piggyback basin.

Given this chronologic framework, rates of shortening can be calculated based on bed-length balancing of the competent lithologic units. In a northwest-southeast transect perpendicular to the traces of the breakback imbricates (Fig. 4), a total of 4.5 km of shortening can be documented with ~3.5 km accommodated by the imbricate thrusts and ~1 km accommodated by the Vilada anticline (Burbank and others, 1990). These data yield a shortening rate of ~0.6 mm/yr for 7.5 m.y. This transect is not, however, parallel to the north-south transport direction of the thrusts (Vergés and Martínez, 1988). If the imbricates are traced westward to a frontal position with respect to their transport direction, they can be shown to accommodate ~18 km of orthogonal shortening at a mean rate of 2.4 mm/yr.

tive with the Artés Formation in the Vic region. Progressive unconformities within these conglomerates (Riba, 1976) indicate that the Vallfogona thrust was active again after ~39.5 Ma.

The cross-cutting stratigraphic and structural relationships among strata of the Ripoll syncline and the Pedraforca thrust sheets permit unusu-

ally tight limits to be placed on the succession of hindward-imbricating thrusts and coeval piggyback thrusts. The magnetic dates on these thrusts suggest that the entire sequence developed over an ~7.5-m.y. span. During this time, deformation appears to have occurred in pulses of rapid thrusting (or anticlinal growth) that generated

The style of deformation of the thrusts bounding the Ripoll basin is strikingly similar to that seen along the eastern margin of the South-Central Unit (Figs. 1 and 2) in the vicinity of the Oliana anticline (Vergés and Muñoz, 1990; Burbank and others, 1992). In both cases,

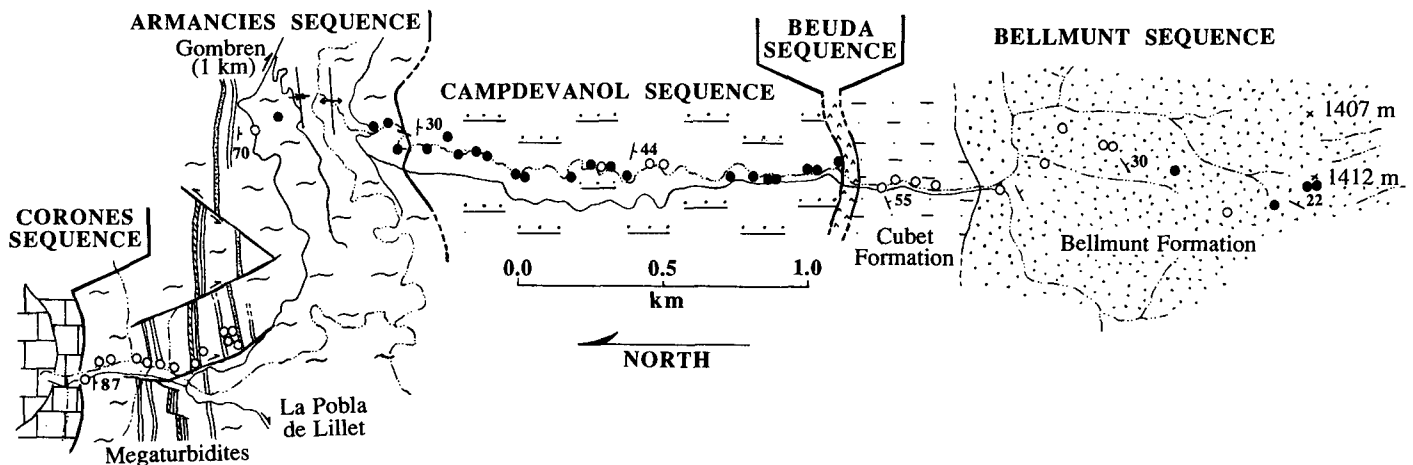


Figure 13. Location map for the Gombren section based on 1:5,000 maps and aerial photographs. Tracing of megaturbidites was used to correlate within the Armànies sequence. See Figure 2 for section location.

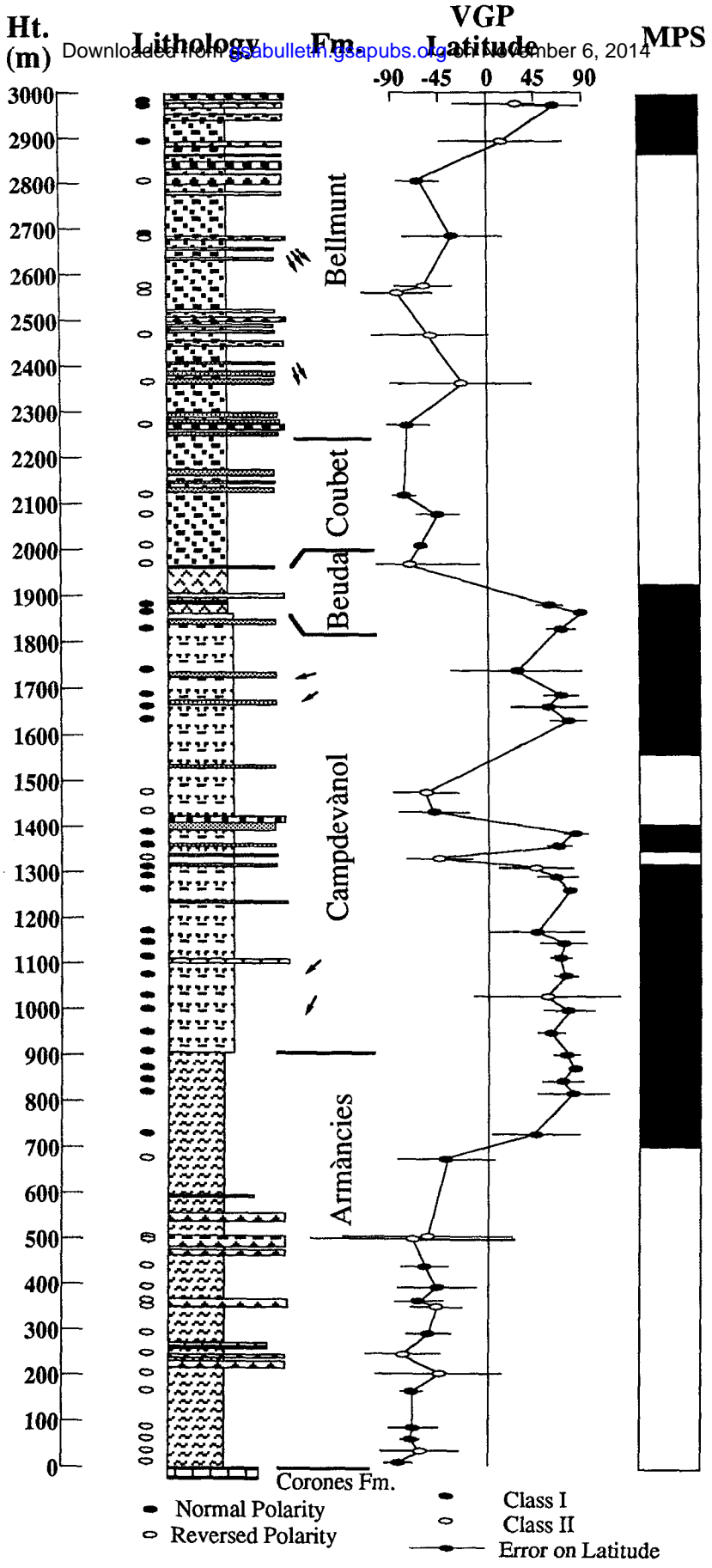
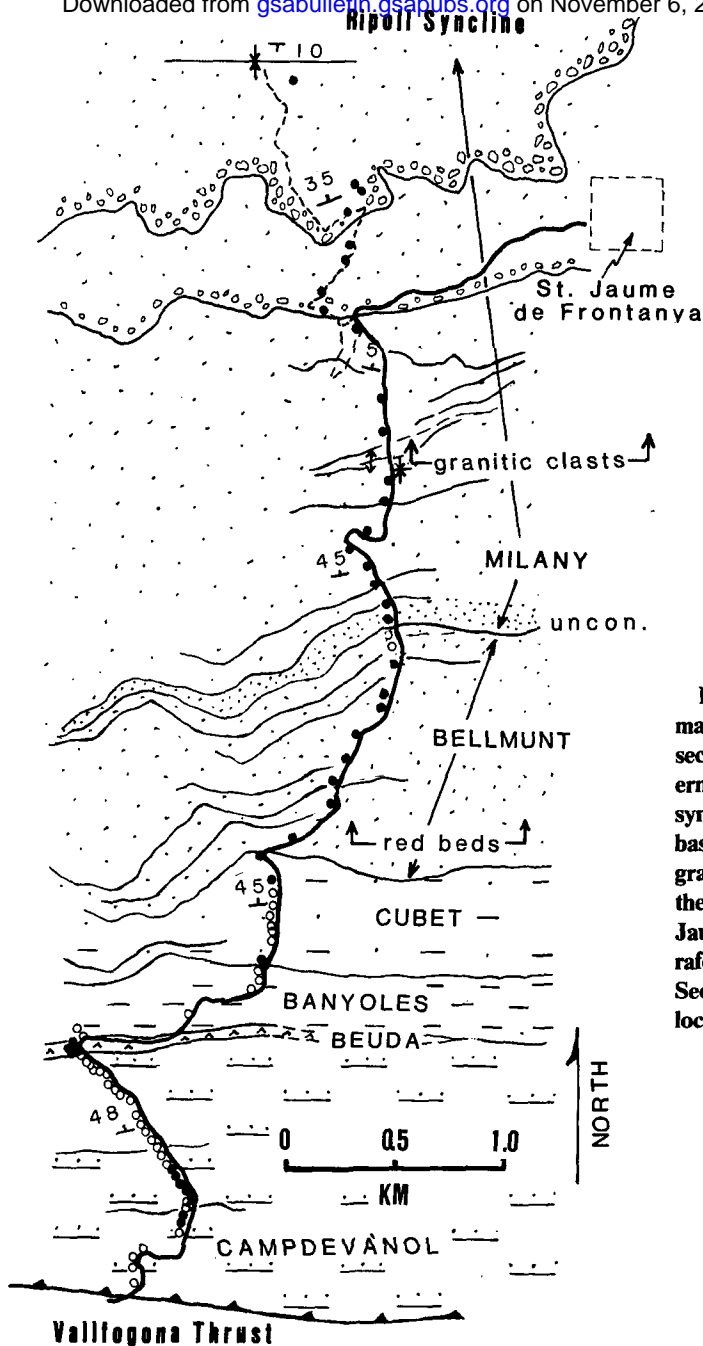


Figure 14. The Gombren MPS. Small arrows indicate paleocurrent directions in the turbidites and in the terrestrial sandstones. For description of symbols, see Figure 8.

Downloaded from [gsabulletin.gsapubs.org](http://gsabulletin.gsapubs.org) on November 6, 2014



**Figure 15.** Location map for the St. Jaume section along the southern limb of the Ripoll syncline. Sample locations based on aerial photographs. See Figure 4 for the relationship of the St. Jaume section to the Pedraforca breakback thrusts. See Figure 2 for section location.

breakback and piggyback thrusting are occurring simultaneously and in close proximity to each other. Both deformed regions are located along oblique ramps, and both exhibit a counterclockwise rotation of the footwall strata in apparent response to the shear couple developed along the oblique thrust-sheet boundary.

The magnetic data (Fig. 6D) indicate that a counterclockwise rotation of the southern Ripoll basin took place during thrusting (Table 1). Pre-Beuda strata are rotated by  $\sim 15^\circ$ , whereas post-

Coubet strata are only rotated  $\sim 5^\circ$ . The intervening strata exhibit intermediate amounts of rotation. The driving force for the rotation is likely to have been the thrusting along the oblique margin of the Pedraforca thrust sheet. Sinistral shear along this ramp between 46 Ma and 47.5 Ma apparently controlled most of the rotation. Perhaps due to its greater distance from the thrusts, the Gombren section on the north side of the syncline shows negligible rotation at this time.

The granitic provenance that characterizes the Milany sequence, including the Folgueroles sandstone in the south, suggests that major, out-of-sequence thrusts (for example, the Ribes-Camprodon thrust; Puigdefàbregas and others, 1986) brought crystalline rocks to the surface to the north of the study area (Freser Valley) at this time. In the upper part of the St. Jaume section, granitic clasts begin appearing in abundance at  $\sim 41.8$  Ma. The glauconite-bearing, transgressive Folgueroles sandstone is dated as spanning  $\sim 42.3$ – $43.9$  Ma (Fig. 9) and appears to correlate with a significant interval of rising sea level (Haq and others, 1987). The overlying Milany sequence at Vic (comprising primarily marl; Fig. 8) is punctuated by two deltaic, southward-prograding sandbodies. The older Oris sandstone at  $\sim 41.5$  Ma is succeeded 0.5 m.y. later by the deltaic sandstone and restricted reefs of the St. Martí Xic complex (Figs. 8 and 17) (Barnolas and others, 1981). Despite the overall shallowing-upward sequence at Vic, subsidence rates generally accelerate over this interval (Fig. 10). Marked rate increases, from  $\sim 10$  cm/ky between 44.5 Ma and 42.5 Ma to  $\sim 60$ – $70$  cm/ky, occur at  $\sim 42.7$  Ma, whereas an apparent deceleration to  $\sim 40$  cm/ky occurs beginning at  $\sim 41.2$  Ma. Enhanced subsidence appears linked to the southward migration of both the locus of thrusting and the foreland depocenter (Puigdefàbregas and others, 1986). Although the Vallfogona thrust was active at this time and an additional thrust load was being emplaced, the Vallfogona thrust involves only cover rocks, and it probably did not generate very large new loads. Instead, it is more likely that major basement-involved thrusts, like those facilitating the emplacement of the lower basement units of the Freser Valley antiformal stack and the Ribes-Camprodon out-of-sequence thrust (Muñoz, 1985; Puigdefàbregas and others, 1986), were active at this time.

As with the sequences farther to the north, the rate decreases (Fig. 10) at Vic (after  $\sim 41$  Ma) are associated with evaporite deposition (Figs. 3 and 17). The age of the Cardona evaporite (Fig. 8) appears to coincide with the timing of the largest, most abrupt sea-level drop recorded during late Eocene to Oligocene times (Haq and others, 1987).

Of the previously described structural events, only the breakback thrusting, the growth of the Vilada anticline, and three intervals of Vallfogona thrusting can be unambiguously dated using cross-cutting relationships that can be clearly related to the studied sections. The timing of other events, such as out-of-sequence thrusting, must be inferred from subsidence records and stratigraphic indicators of tectonism. Nonetheless, these new chronologic data pro-

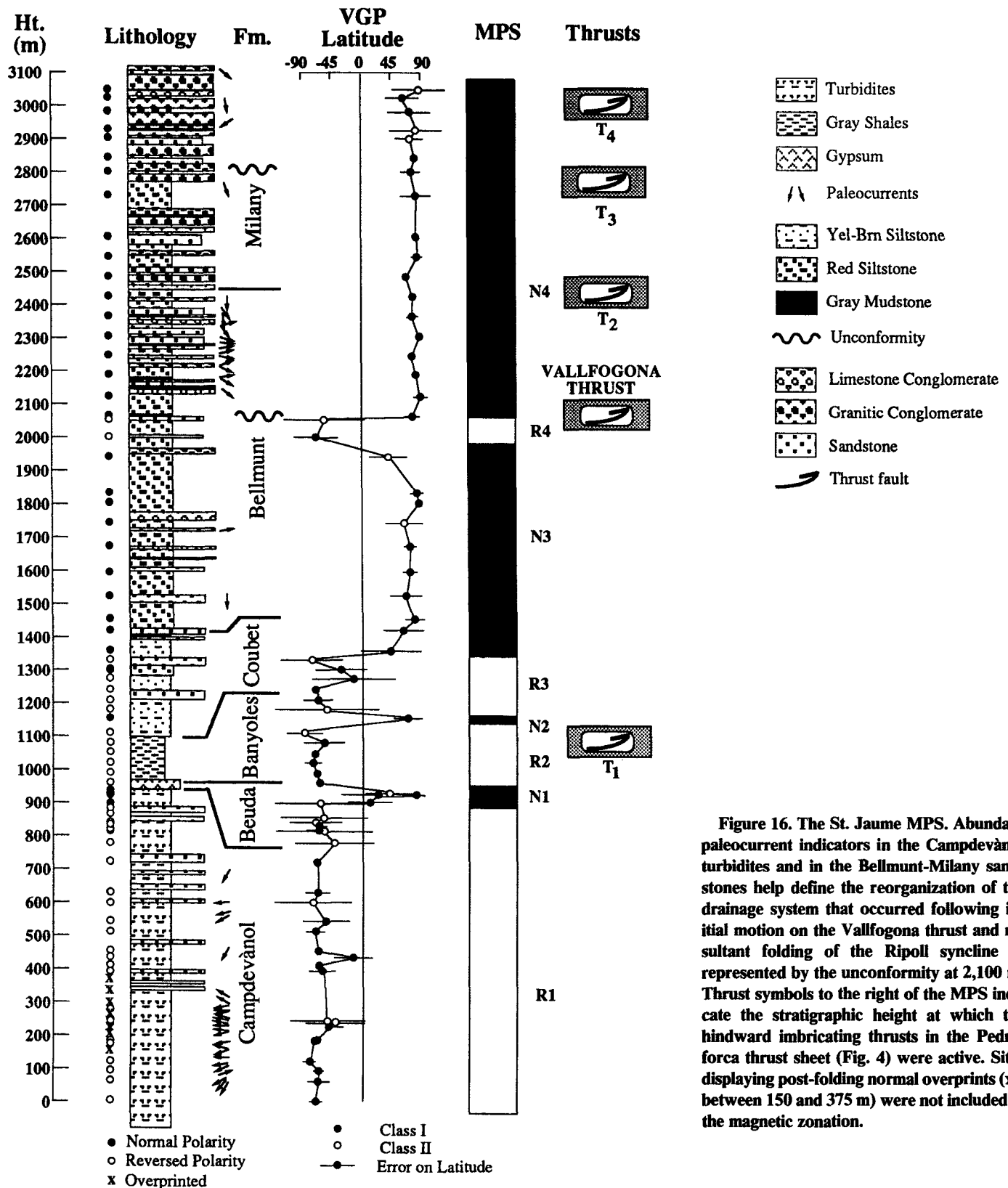


Figure 16. The St. Jaime MPS. Abundant paleocurrent indicators in the Campdevàdol turbidites and in the Bellmunt-Milany sandstones help define the reorganization of the drainage system that occurred following initial motion on the Vallfogona thrust and resultant folding of the Ripoll syncline as represented by the unconformity at 2,100 m. Thrust symbols to the right of the MPS indicate the stratigraphic height at which the hindward imbricating thrusts in the Pedraforca thrust sheet (Fig. 4) were active. Sites displaying post-folding normal overprints (x's between 150 and 375 m) were not included in the magnetic zonation.

## MPTS DATED SEQUENCES AND FORMATIONS TECTONIC HISTORY

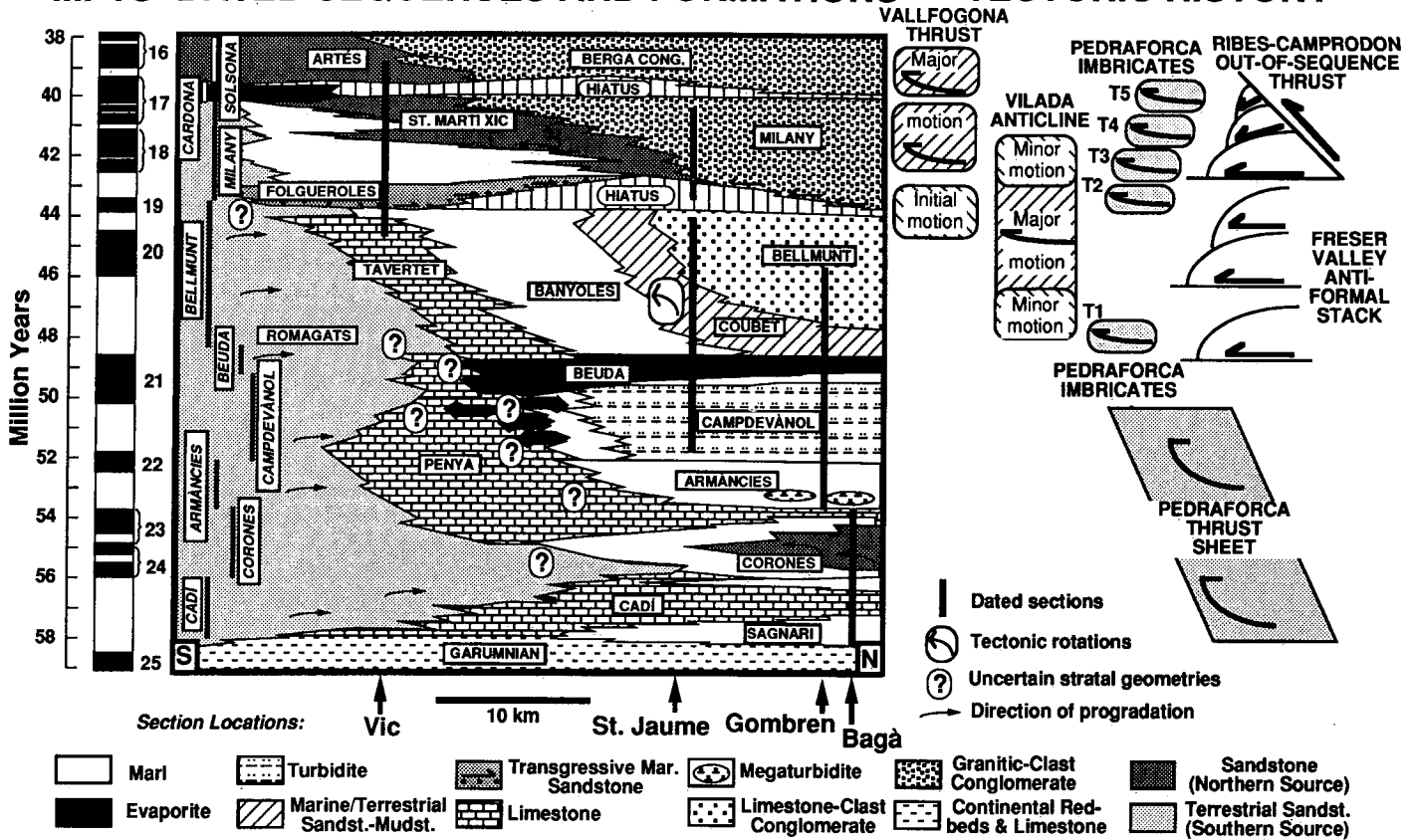


Figure 17. Summary figure of the sedimentation, chronology, and tectonics along a north-south transect of the eastern Pyrenean foreland basin during the Eocene. The location of each of the studied sections is projected orthogonally as much as 10 km onto the transect. Heavy vertical bars represent the temporal extent of the magnetic sections as defined in Figure 9, and within them, the ages of lithologic contacts are well constrained. Between sections, lithologic boundaries are drawn to conform with the available stratigraphic control. The labeled vertical bars on the left represent the time encompassed by each of the nine sequences (see Fig. 3) dated within the study area. The tectonic history of the studied region is summarized on the right. The timing of each Pedraforca imbricate, the growth of the Vilada anticline, and the initial Vallfogona thrusting is specified directly by dating in the St. Jaume section based on the map relationships illustrated by Martínez and others (1988; Fig. 4). The timing of other tectonic events is inferred from the age of the stratigraphic indicators inferred to be responses to thrusting events.

vide a significantly improved temporal framework for continuing analysis of the Pyrenean foreland.

### Relationship to Foreland-Basin Models

Recent models of foreland-basin sedimentation (Flemings and Jordan, 1989, 1990; Angevine and others, 1990) suggest that the patterns of sedimentary infilling of a flexural basin should respond to rather complex interactions among subsidence, sediment supply, base-level change, transport efficiency, and sorting. These factors, in turn, represent responses to changes in loading, erosion, uplift, climate, lithology of source terrains, and sea level. Although many of these controls are poorly known with respect to the Pyrenees at present, some model predictions

(Angevine and others, 1990) regarding grain-size changes and subsidence rates can be examined: in supply-driven basins, progradation of coarse-grained facies should occur during times of accelerated sediment accumulation, whereas in subsidence-driven basins, progradation should occur during times of decreased subsidence and sediment accumulation.

In all four sections described here, decreases in the rate of subsidence are associated with progradation of coarse-grained facies. The uncertainties inherently associated with the subsidence calculations suggest that little significance should be attached to subtle rate changes. Consequently, only large-scale changes are considered here. The Corones red beds (Bagà), the Folgueroles sandstone and Artés red beds (Vic), and the Bellmunt-Milany red beds (Gombren

and St. Jaume) each appear in these sections during or shortly after rates of both subsidence and sediment accumulation decrease (Fig. 10). Because only one of these coarse-grained facies (Corones red beds) appears to be associated with a significant drop in sea level (Haq and others, 1987), these observations suggest that progradation was controlled primarily by subsidence, rather than sediment supply or base-level changes.

In the marine records from Bagà, Gombren, and Vic, accelerating subsidence is associated with a change to finer-grained, largely marly deposition. This tendency agrees with the prediction that, during times of rapid subsidence, coarser sediments will be trapped in the rapidly created space along the proximal basin margin, whereas finer-grained deposition will dominate

in more distal areas. Increases in water depth that are independent of sea-level rises are also associated with these subsidence increases and suggest that the rate of sediment supply could not keep pace with the rate of subsidence.

A contrasting response appears at St. Jaume where, despite the unconformity between 42.5 Ma and 44 Ma, clearly accelerated subsidence (Fig. 10) is associated with increasingly coarse-grained deposition (Fig. 16). This seems to provide an example of a supply-driven progradation. Its occurrence here is not unexpected, because the section is proximal to an imbricating and newly emergent thrust load (Fig. 4). The contention that this hindward-imbricated zone is responsible for a high sediment flux, rather than a more northerly source area, is reinforced by the rather ubiquitous easterly directed paleocurrents in these coarse-grained units (Fig. 16). It may also be important that the Vilada anticline (Fig. 4), which would be likely to have formed a partial barrier to west-east transport, had largely stopped growing by this point.

Foreland-basin models (Flemings and Jordan, 1989, 1990) suggest that subsidence curves can be interpreted in terms of emplacement of thrust loads, such that new loads should accelerate subsidence through much of the basin and cause the greatest subsidence in proximal sites. For example, accelerated subsidence recorded in the Vic section (Fig. 10) apparently reflects an increase in the tectonic load due to piling up of basement units in the antiformal stack and out-of-sequence thrusting in the hinterland (Fig. 2). Similarly, the rapid subsidence during Sagnari deposition is likely to correspond to initial tectonic loading by the Pedraforca thrust sheet (Pujadas and others, 1989).

Recent modeling studies (Zoetemeijer and others, 1990) suggest an effective elastic thickness of ~30 km for the lithosphere beneath the Pyrenees at present. If a similar condition prevailed during Paleogene times, the flexural rigidity would be  $\sim 1.6 \times 10^{23}$  N-m and the basin half width would be ~230 km. In theory, this entire width should be affected by events of thrust loading. For example, during stacking of basement units, the foreland depocenter is likely to have stepped northward due to enhanced subsidence, as predicted by several models (Sinclair and others, 1991; Flemings and Jordan, 1990). Because the Pyrenean foreland basin is partitioned by east-west-oriented thrusts, however, a predictably changing subsidence pattern is not always observed. Thus, although basement thrusting in Milanly times drives a general increase in subsidence in much of the foreland, the Vallfogona thrust is active within the foreland during part of this time, and it creates local thinning and unconformities. These characteristics

might explain apparent enigmas in the stratigraphic and subsidence data.

It is noteworthy that the hindward imbrication of the Pedraforca thrust sheets does not produce a clear subsidence response in the nearby and clearly coeval strata of the Ripoll syncline (Fig. 10). Foreland-basin models indicate that, given their proximity to the thrusts, they should have subsided quickly in response to new loads. Failure to do this, except after 42.5 Ma, may indicate some combination of rapid erosion of the thrust sheets (hence, little new load on the crust; Burbank and Beck, 1991) and activity along the Vallfogona sole thrust that would have translated the basin into a hanging-wall position beginning at 44 Ma—a situation that few forward models have yet addressed.

## CONCLUSIONS

Four new magnetostratigraphic sections, spanning most of Eocene time, have been utilized to improve time constraints on the depositional sequences in the foreland basin of the eastern Pyrenees. These data support the following conclusions.

1. Widespread transgression began by ~58 Ma, as nummulitic limestone was deposited during the next 1 m.y. across much of the eastern Pyrenees. At the same time, marl accumulated in a rapidly subsiding trough caused by initial loading by the Empordà thrust sheet (Pujadas and others, 1989), the eastern equivalent of the Pedraforca thrust sheet.

2. Slowly accumulating, thrust-derived red beds prograded across the region between 56 Ma and 54 Ma (Corones Formation), and major thrusting and rapid subsidence occurred between 53.9 Ma and ~52–50.5 Ma as the Armànies and Campdevànol sequences accumulated.

3. Basin constriction and evaporite deposition (Beuda Formation) mark the end of the initial phase of Pedraforca thrusting at 49–50 Ma.

4. Hindward imbrication of the Pedraforca thrust sheet (Martínez and others, 1988) occurred over a 7.5-m.y. span commencing at 47.5 Ma. Sinistral shearing along the oblique margin of the breakback thrusts caused rotation of footwall strata between 46 Ma and 47.5 Ma. Within the imbricate thrusts, ~18 km of orthogonal shortening occurred at a mean rate of 2.4 mm/yr.

5. Initial movement of the Vallfogona thrust from 42.5 Ma to 44 Ma at ~3 mm/yr caused folding of the Ripoll syncline about an east-west axis and translated the syncline into its hanging wall.

6. To the south of the Ripoll syncline, deposi-

tion on the Tavertet carbonate platform ceased ~44.5 Ma, and the Folgueroles sandstone transgressed across the region between 42.5 Ma and 44.0 Ma. Renewed Vallfogona thrusting deformed Folgueroles rocks from 42 Ma to 40 Ma.

7. Accelerated subsidence near Vic at 42 Ma led primarily to marl deposition over the succeeding 2.5 m.y. This subsidence is a likely response to loading in the hinterland by the antiformal stack and the Ribes-Camprodon thrust sheet. A second episode of basin constriction and evaporite deposition (Cardona sequence) occurred at ~40 Ma.

8. A third interval of Vallfogona thrusting deformed the Berga conglomerate after 39.5 Ma.

9. Following the initial transgression in early Eocene time, the eastern Pyrenean depocenter migrated ~80 km southward at a mean rate of 5 mm/yr over the next 16 m.y.

10. The improved chronologic data indicate that many facies boundaries are time transgressive. Across the relatively narrow width of the Ripoll syncline, the bases of Coubet and Bellmunt sequences apparently vary by as much as 0.5–1.0 m.y. in age and reflect the pace of progradation in this region.

11. Deposition of evaporitic strata, as well as several unconformities or condensed sections, appear to correlate with marked sea-level falls during Eocene times.

12. Regional subsidence is driven primarily by thrust loads involving basement units, and subsidence induced by emergent cover thrust sheets is usually of minor significance.

13. Within the context of recent models for foreland basins, changes in rates of subsidence appear to be primary controls on coarsening and fining trends in the dated stratigraphic record. Direct correlations between stratigraphically recorded thrusting events and synchronous intervals of accelerating subsidence are generally weak. This may, however, be an indication of predictable responses in regions not immediately adjacent to the thrusts themselves.

## ACKNOWLEDGMENTS

This research was supported by National Science Foundation Grants EAR-8517482 and EAR 8816181. Acknowledgment is gratefully made to the donors of the Petroleum Research Fund, administered by the American Chemical Society (grants ACS-PRF 20591 and PRF 17625 to D. W. Burbank). Discussions with Jaume Vergés, Albert Martínez, Josep Serra-Kiel, and Steve Lund have greatly enhanced this work. The careful work of Karen Young in the USC paleomagnetism lab is gratefully acknowledged. Stereonet programs were generously provided by Rick Allmendinger.

## REFERENCES CITED

- Angevine, C. L., Heller, P. L., and Paola, C., 1990, Quantitative sedimentary basin modelling: American Association of Petroleum Geologists Short Course Notes, 133 p.
- Aubry, M. P., 1985, Northwestern European Paleogene magnetostratigraphy, biostratigraphy, and paleogeography: *Calcareous nanofossil evidence: Geology*, v. 13, p. 198–202.
- Barnolas, A., Busquets, P., and Serra-Kiel, J., 1981, Características sedimentológicas de la terminación del ciclo marino del Eoceno superior en el sector oriental de la Depresión del Ebro (Cataluña, NE España): *Acta Geológica Hispánica*, v. 16, p. 215–221.
- Barnolas, A., Samsó, J. M., Teixell, A., Tosquella, J., and Zamorano, M., 1991, Evolución sedimentaria entre la cuenca Graus-Tremp y la cuenca de Jaca-Pamplona: I Congreso del Grupo español del Terciario, Libro-Guía 1, 123 p.
- Berastegui, X., García Senz, J. M., and Losantos, M., 1990, Tectono-sedimentary evolution of the Organyà extensional basin (Central South Pyrenean Unit, Spain) during the Lower Cretaceous: *Bulletin Société Géologique de France*, v. 8, p. 251–264.
- Berggren, W. A., and Kent, D. V., 1989, Late Paleogene time-scale: An update: *Geological Society of America Abstracts with Programs*, v. 21, p. 86.
- Berggren, W. A., Kent, D. V., Flynn, J. J., and van Couvering, J. A., 1985, Cenozoic geochronology: *Geological Society of America Bulletin*, v. 96, p. 1407–1418.
- Burbank, D. W., and Beck, R. A., 1991, Rapid, long-term rates of denudation: *Geology*, v. 19, no. 12, p. 1169–1172.
- Burbank, D. W., and Puigdefàbregas, C., 1985, Chronologic investigations of the South Pyrenean basins: Preliminary magnetostratigraphic results from the Ripoll Basin: International Association of Sedimentologists Sixth European Regional Meeting Abstracts and Poster Abstracts, Lleida, Spain, p. 66–69.
- Burbank, D. W., Vergés, J., and Muñoz, J. A., 1990, Eocene thrusting and rates of shortening along oblique ramps in the central and eastern Pyrenees: *Geological Society of America Abstracts with Programs*, v. 22, p. 98.
- Burbank, D. W., Vergés, J., Muñoz, J. A., and Bentham, P., 1992, Coeval hindward- and forward-imbicating thrusting in the south-central Pyrenees, Spain: Timing and rates of shortening and deposition: *Geological Society of America Bulletin*, v. 104, no. 1, p. 3–17.
- Estevez, A., 1973, La vertiente meridional del Pirineo Catalán al N del curso medio del río Fluvià [Ph.D. dissert.]: Granada, Spain, University of Granada, 514 p.
- Ferrer, J., 1971, El Paleoceno y Eoceno del Borde Sureste de la Depresión del Ebro: *Memoires Suisses de Paléontologie*, v. 90, 70 p.
- Fisher, R. A., 1953, Dispersion on a sphere: *Proceedings of the Royal Society of London*, v. A217, p. 295–305.
- Flemings, P. B., and Jordan, T. E., 1989, A synthetic stratigraphic model of foreland basin development: *Journal of Geophysical Research*, v. 94, p. 3851–3866.
- , 1990, Stratigraphic modeling of foreland basins: Interpreting thrust deformation and lithospheric rheology: *Geology*, v. 18, p. 430–434.
- Garrison, R. E., and Ramirez, P. C., 1989, Conglomerates and breccias in the Monterey Formation and related units as reflections of basin margin history, in Colburn, I. P., Abbott, P. L., and Minch, J., eds., *Conglomerates in basin analysis: A symposium dedicated to A. O. Woodford: Society of Economic Paleontologists and Mineralogists, Pacific Section*, p. 189–206.
- Gich, M., 1972, Estudio geológico del Eoceno prepirenaico del Ripollés oriental [Ph.D. dissert.]: Barcelona, Spain, University of Barcelona, 447 p.
- Guidish, T. M., Kendall, C.G.St.C., Lerche, I., Toth, D. J., and Yarzab, R. F., 1985, Basin evaluation using burial history calculations: An overview: American Association of Petroleum Geologists Bulletin, v. 69, p. 92–105.
- Haq, B. U., Hardenbol, J., and Vail, P. R., 1987, Chronology of fluctuating sea levels since the Triassic: *Science*, v. 235, p. 1156–1167.
- Harland, W. B., Armstrong, R. L., Cox, A. V., Craig, L. E., Smith, A. G., and Smith, D. G., 1990, *A geologic time scale 1989*: Cambridge, England, Cambridge University Press, 263 p.
- Martínez, A., Vergés, J., and Muñoz, J. A., 1988, Secuencias de propagación del sistema de cabalgamientos de la terminación oriental del manto del Pedraforca y relación con los conglomerados sinorogénicos: *Acta Geológica Hispánica*, v. 23, p. 119–128.
- Masson, D. G., and Miles, P. R., 1984, Mesozoic seafloor spreading between Iberia, Europe and North America: *Marine Geology*, v. 56, p. 279–287.
- McElhinny, M. W., 1964, Statistical significance of the fold test in paleomagnetism: *Geophysical Journal of the Royal Astronomical Society*, v. 8, p. 328–340.
- McIntosh, W. C., 1988, Progress toward calibration of mid-Tertiary geomagnetic polarity history using high-precision <sup>40</sup>Ar–<sup>39</sup>Ar geochronology of ignimbrite sequences in SW New Mexico: *Geological Society of America Abstracts with Programs*, v. 21, p. 65–66.
- Mey, P.H.W., Nagtegaal, P.J.C., Roberti, K. J., and Hartvelt, J.J.A., 1968, Lithostratigraphic subdivision of post-Hercynian deposits in the south-central Pyrenees, Spain: *Leidsche Geologische Mededelingen* 41, p. 221–228.
- Montanari, A., DePaulo, D. J., Alvarez, W., Drake, R., Curtis, G. H., Odín, G. S., Turrin, B., and Bice, D. M., 1989, Radio-isotopic calibration of the upper Eocene and Oligocene magnetic polarity and foraminiferal time scales in the northern Apennines of Italy: *Geological Society of America Abstracts with Programs*, v. 21, p. 178.
- Moya, S., Ramos-Guerrero, E., Agustí, J., Checa, L., Köler, M., and Busquets, P., 1991, Depósitos lacustres-palustres asociados a las zonas intermedias de la Fm. Bellmunt (Prepirineo Catalán): I Congreso del Grupo Español del Terciario Comunicaciones, p. 225–228.
- Muñoz, J. A., 1985, Estructura alpina i hercínica a la vora sud de la zona axial del Pirineu oriental [Ph.D. dissert.]: Barcelona, Spain, University of Barcelona, 305 p.
- , 1992, Evolution of a continental collision belt: ECORS-Pyrenees crustal balanced cross-section, in McClay, K., ed., *Thrust tectonics*: London, England, Chapman and Hall, p. 235–246.
- Muñoz, J. A., Martínez, A., and Vergés, J., 1986, Thrust sequences in the Spanish eastern Pyrenees: *Journal of Structural Geology*, v. 8, p. 399–405.
- Ortí, F., Busquets, P., and Rosell, L., 1985, Estudi petrològic, sedimentològic i estratigràfic de la conca evaporítica catalana de l'Eocè Mitjà—(Lutecia), *Memòria de l'Ajut d'investigació* (1983): Barcelona, Spain, University of Barcelona, 34 p.
- Parés, J.-M., Banda, E., and Santanach, P., 1988, Paleomagnetic results from the southeastern margin of the Ebro Basin (NE Spain): *Physics of Earth and Planetary Interiors*, v. 52, p. 267–282.
- Powers, M.M.K., 1989, Magnetostratigraphy and rock magnetism of Eocene foreland basin sediments, Esera and Isabena River valleys, Tremp-Graus basin, southern Pyrenees, Spain [M.S. thesis]: Los Angeles, California, University of Southern California, 225 p.
- Puigdefàbregas, C., and Souquet, P., 1986, Tectono-sedimentary cycles and depositional sequences of the Mesozoic and Tertiary from the Pyrenees: *Tectonophysics*, v. 129, p. 173–203.
- Puigdefàbregas, C., Muñoz, J. A., and Marzo, M., 1986, Thrust belt development in the Eastern Pyrenees and related depositional sequences in the southern foreland basin, in Allen, P. A., and Homewood, P., eds., *Foreland basins: Special Publication International Association of Sedimentologists*, no. 8, p. 229–246.
- Pujadas, J., Casas, J. M., Muñoz, J. A., and Sabat, F., 1989, Thrust tectonics and paleogene syntectonic sedimentation in the Empordà area, south-eastern Pyrenees: *Geodinamica Acta*, v. 3, p. 195–206.
- Reguant, S., 1967, El Eoceno marino de Vic (Barcelona): *Memoir Institut Geològic i Mineral de España*, no. 68, 330 p.
- Riba, O., 1976, Syntectonic unconformities of the Alto Cardener, Spanish Pyrenees: A genetic interpretation: *Sedimentary Geology*, v. 15, p. 213–233.
- Rios, J. M., and Masachs, 1953, Hoja 295 (Bañolas) del Mapa Geológico de España, escala 1:50,000: *Investigaciones de Geología y Minerales de España*.
- Sáez, A., Vergés, J., Taberner, C., Pueyo, J. J., Muñoz, J. A., and Busquets, P., 1991, Eventos evaporíticos paleógenos en la cuenca de antepais surpirenaica: ¿Causas climáticas—causas tectónicas?: I Congreso del Grupo español del Terciario, Libro-Guía 5, 85 p.
- Slater, J. G., and Christie, R.A.F., 1980, Continental stretching: An explanation of the post-Mid-Cretaceous subsidence of the Central North Sea Basin: *Journal of Geophysical Research*, v. 85, p. 711–739.
- Séguret, M., Labaume, P., and Madriaga, P., 1984, Eocene seismicity in the Pyrenees from megaturbidites of the South Pyrenean Basin (Spain): *Marine Geology*, v. 55, p. 117–131.
- Serra-Kiel, J., 1981, Estudi sobre la sistemàtica filogenètica, biostratigràfica i paleobiologia dels Nummulites del grup N. pernotus, N. perforatus—(conca aquitana, catalana i balear) [Ph.D. dissert.]: Barcelona, Spain, University of Barcelona, 543 p.
- Simo, A., 1986, Carbonate platform depositional sequence, upper Cretaceous, south-central Pyrenees (Spain): *Tectonophysics*, v. 129, p. 205–231.
- Sinclair, H. D., Coakley, B. J., Allen, P. A., and Watts, A. B., 1991, Simulation of foreland basin stratigraphy using a diffusion model of mountain belt uplift and erosion: An example from the Central Alps, Switzerland: *Tectonics*, v. 10, p. 599–620.
- Steckler, M. S., and Watts, A. B., 1978, Subsidence of the Atlantic type continental margin off New York: *Earth and Planetary Science Letters*, v. 42, p. 1–13.
- Van Eeckhout, J. A., 1990, Estratigrafia i sedimentologia de la Formació de Vallfogona entre los Rios Llobregat y Ter [M.S. thesis]: Barcelona, Spain, University of Barcelona, 104 p.
- Vergés, J., and Martínez, A., 1988, Corte compensado del Pirineo oriental: Geometría de las cuencas de antepais y edades de emplazamiento de los mantos de corrimiento: *Acta Geológica Hispánica*, v. 23, p. 95–105.
- Vergés, J., and Muñoz, J. A., 1990, Thrust sequences in the southern central Pyrenees: *Bulletin de la Société Géologique de France*, v. 8, p. 399–405.
- Zoetemeijer, R., Desegaulx, P., Cloetingh, S., Roure, F., and Moretti, I., 1990, Lithospheric dynamics and tectonic-stratigraphic evolution of the Ebro Basin: *Journal of Geophysical Research*, v. 95, p. 2701–2711.

MANUSCRIPT RECEIVED BY THE SOCIETY DECEMBER 19, 1990

REVISED MANUSCRIPT RECEIVED DECEMBER 4, 1991

MANUSCRIPT ACCEPTED DECEMBER 11, 1991